Study on key determinants of Raloxifene and its glucuronide disposition

2015

Keigo Kosaka

CONTENTS

Introduction

Glucuronidation is a phase II metabolic reaction catalyzed by UDP-glucuronosyltransferase (UGT) that transforms endogenous substances and xenobiotics into more hydrophilic compounds that are subsequently eliminated through excretion of urine and/or bile. Most lipophilic drugs are initially metabolized by cytochrome P450 (P450). Therefore, during the discovery stage of new chemical entities (NCEs), pharmaceutical companies focus more on preventing the metabolism of these drugs by P450. However, over the last decade, more hydrophilic compounds have been synthesized, and new concerns regarding UGT-catalyzed metabolism have been revealed because these processes are important for detoxification and prolongation of efficacy of some drugs. UGTs are widely expressed in various tissues including the liver, kidney, and gastrointestinal tract, implying that extrahepatic metabolism may exert a critical influence on the pharmacokinetics of glucuronidated drugs. It is well known that phenolic compounds including opioid analgesics such as morphine and flavonoids are extensively glucuronidated in the liver and small intestine (Ritter, 2007). In some cases, poor oral bioavailability (F) of the drugs is attributed to the susceptibilities to glucuronidation. Therefore, extrapolation of in vitro glucuronidation data to in vivo pharmacokinetic parameters is essential but difficult because of the complex nature of UGT enzymes (Lin and Wong, 2002). Several studies on in vitro-in vivo correlation (IVIVC) for UGT substrates have been published recently (Kilford et al., 2009; Miners et al., 2010). It was reported that in vitro predictability depends on enzyme sources, experimental conditions, and the occurrence of atypical glucuronidation kinetics, and thus selection of an appropriate approach is a key point to predict pharmacokinetics successfully. In the chapter I, intestinal and hepatic glucuronidation of four compounds including raloxifene, which are mainly eliminated through glucuronidation, were examined by microsomal incubation and compared with in vivo clearances. The product of fraction absorbed and intestinal availability (Fa·Fg) and hepatic availability (Fh) of the four compounds were estimated in rats by monitoring the concentration in the portal and systemic blood after oral administration. Furthermore, to clarify the involvement of Ugt1As

in the glucuronidation of raloxifene, the pharmacokinetic profiles of raloxifene in Ugt1A-deficient rats (Gunn rats) were compared with those of their wild-type (Wistar) rats.

Organic anions such as carboxylic drugs and phase II metabolites are actively transported by organic anion transporting polypeptides (Oatps), multidrug resistance-associated proteins (Mrps), and other transporters. Oatps and Mrps play a major role in sinusoidal uptake, canalicular excretion, and, to some extent, basolateral efflux in the liver. In the drug development process, it is important to know which transporters are involved in the disposition of organic anions in the liver, and ultimately at what level these compounds are systemically exposed. Although interspecies differences in hepatic uptake and biliary excretion of organic anions are common (Soars et al., 2007; Gardiner et al., 2011; Li et al., 2008; Grime et al., 2013), no general rule explaining the differences in the disposition of organic anions between experimental animals and humans has been established. Therefore, extrapolation of pharmacokinetics from preclinical animals to humans is still a challenge for these compounds, particularly if carrier-mediated transport is involved. In the chapter I, a large difference in the systemic exposure of raloxifene glucuronides as major metabolites between Sprague–Dawley (SD) rats and Mrp2-deficient rats, Eisai hyperbilirubinemic rats (EHBRs), was observed: the blood concentration ratio of raloxifene glucuronides to the parent drug was greater in EHBRs (129) than that in SD rats (10). Thus, in the Chapter II, we focused particularly on the pharmacokinetic differences of three organic anions including raloxifene-6-glucuronide (R6G) between SD rats and EHBRs to determine whether they could be explained solely by a difference in its biliary excretion process.

Chapter I

Intestinal and hepatic glucuronidation of raloxifene and the other compounds

I-i. Introduction

Raloxifene is a selective estrogen receptor modulator used for the prevention and treatment of postmenopausal osteoporosis and for the prevention of breast cancer. Its bioavailability (F) in humans has been reported as only 2% (Eli Lilly clinical data, Indianapolis, IN; Mizuma, 2009). UGT1A8 and UGT1A10, isozymes that are absent in the human liver, are thought to glucuronidate raloxifene mainly in the intestine and lead to extremely low F (Kemp et al., 2002; Jeong et al., 2005). F of raloxifene in rats and dogs was originally reported as 39 and 17%, respectively (Lindstrom et al., 1984), and have been recently reported as 4 and 0%, respectively (Deguchi et al., 2011). The Ugt isozymes responsible for the glucuronidation of raloxifene and its intestinal and hepatic availabilities (Fg and Fh, respectively) in preclinical animals have not been investigated adequately. It has been reported that raloxifene and its conjugates were excreted into the bile and gut lumen by P-glycoprotein and/or MRPs, and these efflux transports are considered to participate in the long-lasting enteric recycling of this drug (Jeong et al., 2004; Xu et al., 2009). At present, human UGT isoforms responsible for glucuronidating some drugs are being investigated in detail; however, much less is known about Ugts in animals, species differences in intestinal and hepatic glucuronidation, and subsequent excretion of glucuronides.

In the present study, raloxifene and its glucuronides in the portal and systemic blood were monitored after oral administration in rats and dogs to estimate the contribution of intestinal and hepatic glucuronidation to the first-pass effect. This approach confirmed the species differences in Fa·Fg and Fh of raloxifene. The in vitro intestinal and hepatic intrinsic clearance (CL_{int}) values, which were corrected to $CL_{int, u}$ using microsomal binding in the incubation mixture, were determined using rat, dog, monkey, and human microsomes fortified with UDPGA or NADPH, and the IVIVCs were also examined. To clarify the involvement of Ugt1As in the glucuronidation of raloxifene and the role of Mrp2 in the excretion of its glucuronides, the pharmacokinetic profiles of raloxifene in Gunn rats

and EHBRs were compared with those of their wild-type (Wistar and SD) rats. Furthermore, the IVIVCs of several other compounds (biochanin A, mycophenolic acid, and gemfibrozil), which are mainly eliminated through glucuronidation in rats, were also investigated. The purpose of this study was to examine the usefulness of in vitro microsomal assays of intestinal and hepatic glucuronidation in improving the pharmacokinetic profiles of NCEs during drug discovery.

I-ii. Materials and Methods

Reagents. Raloxifene, β-glucuronidase (type IX-A, from Escherichia coli), glucose 6-phosphate, and NADP were purchased from Sigma-Aldrich (St. Louis, MO). Mycophenolic acid, biochanin A, gemfibrozil, and EDTA were purchased from Wako Pure Chemicals (Osaka, Japan). Glucose-6-phosphate dehydrogenase and protease inhibitor cocktail tablets (Complete, EDTA-free) were purchased from Roche (Mannheim, Germany). The UGT reaction mix solution (250 mM Tris-HCl, 40 mM $MgCl_2$, and 0.125 mg/ml alamethicin) was purchased from BD Gentest (Woburn, MA). Liver and intestinal microsomes from SD rats, beagle dogs, cynomolgus monkeys, and humans were obtained from XenoTech, LLC (Lenexa, KS). All chemicals were analytical grade or the highest quality available.

Animals. All animal procedures were conducted under protocols approved by the Mitsubishi Tanabe Institutional Animal Care and Use Committee. Eight-week-old male Wistar rats, SD rats, Gunn rats, and EHBRs were obtained from Japan SLC (Shizuoka, Japan). Male SD rats (9–10 weeks old) with catheters implanted in the portal and jugular vein were obtained from Charles River Japan (Yokohama, Japan). Rats were kept in a temperature- and humidity-controlled environment and were allowed to acclimate for 1 week before use. Male beagle dogs (7–17 months old) were obtained from Kitayama Labs (Nagano, Japan). Male cynomolgus monkeys (42–61 months old) were obtained from Nafovanny (Dong Nai, Vietnam). These animals were housed in Mitsubishi Chemical Medience facilities where the temperature and humidity were controlled.

Preparation of Microsomes. To compare the metabolic activities of different strains of rats, liver and intestinal microsomes from SD rats, EHBRs, Wistar rats, and Gunn rats were prepared (pooled, n = 3). Rat liver microsomes were prepared using standard techniques (von Moltke et al., 1993). In brief, pooled microsomes from three individuals were prepared by ultracentrifugation (11,900g for 20 min and 104,700g for 1 h twice). Microsomal pellets were resuspended in 0.1 M phosphate-buffered saline (PBS) (pH 7.4) containing 20% glycerol. The total protein concentration was determined using a BCA

Protein Assay Kit (Thermo Fisher Scientific, Waltham, MA) using bovine serum albumin (BSA) as a standard. The prepared microsomes were stored at −80°C until use. Rat intestinal microsomes were prepared as described in a previous study by another group (Perloff et al., 2004). In brief, after exsanguination, 15-cm sections of the upper intestines from the duodenum to the jejunum were immediately isolated, and the intestinal segments were flushed and incubated in solution A (pH 7.3) containing 1.5 mM KCl, 96 mM NaCl, 27 mM sodium citrate, 9.6 mM PBS, and protease inhibitor (20 tablets/l) with bubbling oxygen for 15 min at 4°C. The intestinal segments were filled with solution B (pH 7.0) containing 1.5 mM KCl, 96 mM NaCl, 1.5 mM EDTA, 1 mM dithiothreitol, 0.1% BSA, 9.6 mM PBS, and protease inhibitor (20 tablets/l). After tapping the intestinal segments on an ice-cooled plate for 2 min to peel the epithelial cells off the intestinal wall, the suspension in the lumen was collected. The suspension was centrifuged at 800g for 10 min, and the resulting pellets were resuspended in solution C (pH 7.0) containing 5 mM histidine, 0.25 M sucrose, 0.5 mM EDTA, and protease inhibitor (20 tablets/l). The cell pellets were washed with solution C and homogenized and centrifuged at 15,000g for 10 min. The supernatant was collected, and 5 volumes of 52 mM $CaCl_2$ were added. The tubes containing microsomes were gently mixed, allowed to stand for 15 min, and centrifuged at 2000g for 10 min. The resulting microsomal pellets were suspended in solution D (pH 7.4) containing 20% glycerol, 10 mM EDTA, and 0.1 M Tris-HCl buffer. The total protein concentration was determined by the BCA protein assay, and the microsomes were stored at −80°C until use.

Microsomal Incubation. CL_{int} was determined using the substrate depletion method (n = 3–5). Substrate solutions were prepared at a final concentration of 2 M in dimethyl sulfoxide and acetonitrile (0.01 and 0.99% final concentrations, respectively) except for gemfibrozil (10 M final concentration). The substrates were incubated in 96-well plates and placed on a heating block at 37°C. The suspensions containing microsomes (0.5 mg/ml protein except for biochanin A, 0.1 mg/ml protein) were either dispensed into the 50 mM Tris-HCl solution (pH 7.5) with 25 g/ml alamethicin

8

and 8 mM $MgCl_2$ for UGT reactions or into the 72.5 mM PBS with 5 mM $MgCl_2$ and 1 mM EDTA for P450 reactions as final concentrations. The suspensions were vortexed and allowed to stand for 10 min in the heating block, and the metabolism assay was initiated by addition of 2 mM UDPGA or the NADPHgenerating system containing 1 mM NADP, 10 mM glucose 6-phosphate, and 2 units/ml glucose-6-phosphate dehydrogenase as final concentrations. All assays were incubated for a maximum of 60 min, and reactions were terminated with 4 volumes of acetonitrile containing 0.1% formic acid and verapamil as the internal standard (IS). The samples were then centrifuged, and the supernatant was filtered and transferred to the other 96-well plates for analysis using a liquid chromatography/tandem mass spectrometry (LC-MS/MS) system as described below.

Microsomal Binding. The unbound fraction in rat liver microsomal suspensions ($f_{u,\ mic}$) was determined in triplicate by ultracentrifugation. The microsomes were suspended in 72.5 mM PBS at the same concentration as that used for metabolic stability experiments. The samples for binding studies were centrifuged at 436,000g for 4 h at 37°C, and aliquots of the centrifuged upper fraction were transferred into 15 volumes of acetonitrile containing IS. Standard samples containing the same matrices were prepared, and the unbound compound concentrations in the incubation mixtures were quantified using LC-MS/MS.

Plasma Protein Binding. The unbound fraction in rat plasma ($f_{u,\ p}$) was determined in triplicate by equilibrium dialysis using a serum binding system (BD Gentest). Plasma samples were spiked with the test compound (10 M final concentration), and the device containing plasma and PBS was reciprocated in a CO_2 incubator at 37°C for 20 h. The resulting PBS samples were transferred into 8 volumes of acetonitrile containing IS. Standard samples containing the same matrices were prepared, and the unbound compound concentration in the plasma was quantified using LC-MS/MS.

Blood/Plasma Concentration Ratio. The blood/plasma concentration ratio (R_b) was determined in vitro after incubation of the compounds with fresh rat blood in duplicate. Blood was warmed to 37°C, and the test compound was spiked at a 10 μM final concentration. The blood samples were incubated

at 37°C for 5 min and divided into two portions. After centrifugation of the aliquot, the plasma and blood samples were transferred into 4 volumes of acetonitrile containing IS, centrifuged, and filtered. Standard samples containing the same matrices were prepared, and the compound concentration in plasma and blood was quantified by LC-MS/MS.

Pharmacokinetic Studies in Animals. Raloxifene (1 mg/kg b.wt.) was dissolved in a solution containing ethanol, polyethylene glycol 300, and water (1:4:5) as reported previously (Lindstrom et al., 1984) and administered intravenously at a volume of 0.5 ml/kg to fasted SD rats, Wistar rats, EHBRs, and Gunn rats (n = 3). Blood samples were collected from the animals at 0.05, 0.25, 0.5, 1, 2, 4, 8, and 24 h after dosing. The plasma samples were separated by centrifugation and stored at −20°C. The plasma samples were processed for analysis by protein precipitation with acetonitrile containing IS, followed by centrifugation and filtration. Standard samples containing the same matrices were prepared, and the compound concentrations in the plasma were quantified using LC-MS/MS. For monitoring raloxifene concentrations in portal and systemic plasma after oral administration, SD rats cannulated in the portal and jugular vein were used. Raloxifene (2 mg/kg b.wt.) was dissolved in the same solution as used for intravenous administration at a volume of 4 ml/kg (n = 3–4), and blood samples were collected at 0.25, 0.5, 1, 2, 4, 8, and 24 h after dosing. For monitoring drug concentrations in portal and systemic plasma after oral administration to EHBRs, Wistar rats, and Gunn rats, all animals were sacrificed at five or six time points (n = 3), and blood samples were collected. Intravenous (n = 2) or oral (n = 3) administration of raloxifene to beagle dogs was conducted using the same solution as that administered to the rats, and pharmacokinetic profile studies in cynomolgus monkeys were performed in the same manner (n = 2). When raloxifene was studied in dogs, pharmacokinetic parameters before and after cannulation in the portal vein were compared. The other UGT substrates, biochanin A (50 mg/kg p.o.), mycophenolic acid (10 mg/kg p.o.), and gemfibrozil (30 mg/kg p.o.), were administered to intact SD rats (intravenous) or cannulated SD rats (oral) under the same conditions used for raloxifene (n = 3). The preparation of plasma samples was

as described above except for gemfibrozil, for which the collected plasma samples were immediately transferred to acetonitrile (containing 0.1% formic acid) and IS to avoid degradation of its acyl glucuronide.

Quantification of Glucuronides. The glucuronide concentrations of raloxifene and biochanin A were estimated through a hydrolysis assay using β-glucuronidase. The samples were incubated in the presence of 250 units of β-glucuronidase at 37°C for 12 to 15 h, and the completion of hydrolysis was ascertained by LC-MS/MS analysis. The glucuronide concentration of gemfibrozil was determined by UV detection without a hydrolysis assay, in which it was assumed that the UV absorbances of the unchanged drug and glucuronide were the same. Because only traces of mycophenolic acid glucuronides were detected by UV, these were not quantified.

LC-MS/MS Analysis. Qualitative analysis for the identification of metabolites was performed using an HP1100 system (Agilent Technologies, Santa Clara, CA) equipped with a triple quadrupole Quattro Micro mass spectrometer (Waters, Milford, MA). LC conditions were as follows: column temperature, 40°C; column, CAPCELL PAK MGII (2.0 mm i.d. × 150 mm, 3 μm; Shiseido, Tokyo, Japan); gradient elution at 0.2 ml/min, with acetonitrile and 10 mM ammonium acetate; UV detection, 290 nm; and run time, 20 min. The main working parameters for mass spectrometers were as follows: ion mode, electrospray ionization, positive and negative; capillary voltage, 3 kV; cone voltages, 20 and 40 V; source temperature, 100°C; and desolvation temperature, 350°C. The quantitative analysis for unchanged compounds was performed using an Acquity UPLC system equipped with a triple quadrupole mass spectrometer (Xevo TQ MS; Waters). UPLC conditions were set as follows: column temperature, 50°C; column, Waters Acquity UPLC BEH C18 (2.1 mm i.d. × 30 mm, 1.7 μm); gradient elution at 0.5 ml/min, with acetonitrile and 10 mM ammonium acetate; and run time, 3 min. The parameters for mass spectrometers were as follows: ion mode, electrospray ionization, positive for raloxifene, biochanin A, and mycophenolic acid and negative for gemfibrozil; multireaction monitoring method with transitions of m/z 474 3 112 for raloxifene, m/z 285 3 213 for biochanin A,

m/z 321 3 159 for mycophenolic acid, and m/z 249 3 121 for gemfibrozil; capillary voltage, 0.5 kV; cone voltage and collision energy, 50 V and 30 eV for raloxifene, 50 V and 40 eV for biochanin A, 40 V and 35 eV for mycophenolic acid, and 20 V and 30 eV for gemfibrozil; source temperature, 150°C; and desolvation temperature, 600°C.

Estimation of Fh, Fa·Fg, and F. Fh was calculated by dividing the systemic plasma AUCs (AUCsys) by the portal plasma AUCs (AUCpv) after oral administration to animals. Fa·Fg was estimated using eq. 1:

$$Fa \cdot Fg = Q_{pv} \cdot R_b \cdot (AUCpv - AUCsys) / dose \qquad (1)$$

where Q_{pv} is the blood flow in the portal vein, which was assumed to be 70% of the hepatic blood flow (Q_h) set at 55 ml·min^{-1}·kg^{-1} b.wt. for rats or 31 ml·min^{-1}·kg^{-1} b.wt. for dogs (Davies and Morris, 1993). F was calculated by multiplying Fh and Fa·Fg when AUCpv was available. If AUCpv was not available, F was calculated by dividing the oral AUC by the intravenous AUC normalized with dose.

IVIVC of UGT Substrates in Rats. Data from incubations with either P450 or UGT cofactors were analyzed using a nonlinear single exponential fit, and the CL_{int} values (milliliters per minute per milligram of protein) were calculated from the elimination rate constant k, volume of incubation, and amount of microsomal protein in incubation. CL_{int} values obtained were corrected for experimentally determined $f_{u, mic}$ to give $CL_{int, u}$ and were scaled to the whole-body clearance, $CL_{int, h}$ (milliliters per minute per kilogram body weight) for rats using eq. 2:

$$CL_{int, h} = k \cdot 50 \text{ mg microsomes/g liver} \cdot 37.8 \text{ g liver/kg b.wt. } / \text{ (microsomes concentration} \cdot f_{u,mic}) \qquad (2)$$

where 50 mg of microsomes/g liver was a scaling factor (Iwatsubo et al., 1996; Zhou et al., 2002) and

37.8 g liver/kg b.wt. was the liver weight used (Luttringer et al., 2003). The observed hepatic clearance values after intravenous administration were converted to $CL_{int,\ iv}$ values using the well stirred or parallel tube liver models, defined in eqs. 3 and 4, respectively:

$$\text{Observed } CL_{int,\ iv} = CL_b/f_{u,p} \ \cdot\ R_b/(1 - CL_b/Q_h) \qquad (3)$$

$$\text{Observed } CL_{int,\ iv} = - Q_h/f_{u,p} \ \cdot\ R_b \ \cdot\ \ln(1 - CL_b/Q_h) \qquad (4)$$

where CL_b is the hepatic blood clearance. For biochanin A, the calculated CL_b value exceeded the Q_h, and, therefore, CL_b was assumed to be 90% of the hepatic blood flow as reported previously by another group (Cubitt et al., 2009). The renal clearance of the four compounds used in this study was minor; therefore, hepatic clearance was assumed to be equal to the total clearance. The observed $CL_{int,\ p.o.}$ was calculated from the oral plasma clearance using eq. 5, which assumed complete absorption and no intestinal metabolism:

$$\text{Observed } CL_{int,\ po} = CL_{po}/f_{u,p} \ \cdot\ R_b \qquad (5)$$

I-iii. Results

In Vitro Hepatic and Intestinal Intrinsic Clearance of Raloxifene. The in vitro $CL_{int, u}$ values of raloxifene were estimated using liver and intestinal microsomes (XenoTech, LLC) fortified with NADPH or UDPGA. The final values were corrected with the free fraction in microsomal incubation ($f_{u, mic}$, 0.278) (Table I-1). The in vitro $CL_{int, u}$ values for glucuronidation determined with intestinal microsomes were higher than those with liver microsomes among the tested species, and the values using human intestinal microsomes were the highest. In contrast, the in vitro $CL_{int, u}$ values for P450-catalyzed metabolism were higher with liver microsomes than with intestinal microsomes for these species. The liver and intestinal microsomes were prepared from SD rats, Wistar rats, EHBRs, and Gunn rats, and the in vitro CLint, u values of raloxifene were compared. As expected, the in vitro CLint, u for glucuronidation determined with Gunn rat microsomes was significantly lower than that with Wistar rat microsomes (Figure I-1A). The in vitro CLint, u values for P450 metabolism in EHBRs and Gunn rats were lower than those in SD and Wistar rats, respectively (Figure I-1B).

Pharmacokinetics of Raloxifene. LC-MS/MS analysis with UV detection (290 nm) of the SD rat portal plasma samples at 15 min after oral administration of raloxifene resulted in the appearance of two glucuronide peaks as major metabolites (Figure I-2). Other metabolites such as sulfated or oxidized raloxifene were less. After incubation of this plasma sample in the presence of β-glucuronidase, the two major peaks disappeared. The plasma concentration versus time curves of raloxifene and its glucuronides in SD rats showed rapid absorption and extensive glucuronidation (Figure I-3A). Fa·Fg and Fh in SD rats were estimated to be 0.16 and 0.33, respectively, and the AUC ratio of glucuronides to the unchanged drug was 5.73 and 9.67 in the portal and systemic plasma, respectively (Table I-2). The pharmacokinetics in Gunn and wild-type Wistar rats exhibited significant differences (Figure I-3, B and D). Fa·Fg and Fh in Gunn rats were 0.63 and 0.43, respectively; these values were twice those observed (0.34 and 0.20, respectively) in Wistar rats. The AUC ratio of glucuronides to unchanged drug in the portal plasma was 2.51 in Wistar rats and 0.03 in Gunn rats.

The plasma concentration of raloxifene glucuronides in EHBRs was dramatically higher than that in wild-type SD rats (Figure I-3, A and C). The AUC ratio of glucuronides to unchanged drug in EHBRs was 46.8 in the portal plasma and 129 in the systemic plasma (Table I-2). The PK parameters of raloxifene in beagle dogs were examined before and after implantation of catheters in the portal vein. The total clearance and F were similar before and after the cannulation. $Fa \cdot Fg$ and Fh in dogs were estimated to be 0.36 and 0.16, respectively (Figure I-3E and Table I-2). F in dogs (0.044 and 0.052) was comparable to F in SD rats (0.048), but the AUC ratios of glucuronides to unchanged drug were lower in dogs (portal, 0.27; systemic, 1.34) than in rats (portal, 5.73; systemic, 9.67). F in cynomolgus monkeys was also comparable (0.030) with those in rats and dogs, but the AUC ratios of glucuronides to unchanged drug in systemic plasma were higher in monkeys (85.0) than in rats and dogs (Figure I-3F and Table I-2).

IVIVC of Other UGT Substrates in Rats. The in vitro $CL_{int, u}$ values of biochanin A, mycophenolic acid, and gemfibrozil were determined using rat liver and intestinal microsomes (Table I-3). The $CL_{int, u}$ values of biochanin A for glucuronidation were extremely high in both rat liver and intestinal microsomes. The $CL_{int, u}$ values of mycophenolic acid for glucuronidation were higher in rat intestinal microsomes than in rat liver microsomes. In contrast, $CL_{int, u}$ values of gemfibrozil for glucuronidation were lower in rat intestinal microsomes than in rat liver microsomes. In all cases, the in vitro $CL_{int, u}$ values for P450 metabolism were less than those for glucuronidation. The in vitro hepatic $CL_{int, u}$ values for glucuronidation were scaled to whole-body clearance values (milligrams per minute per kilogram b.wt.) and were compared with the in vivo CL_{int} values obtained from both intravenous and oral pharmacokinetic data (Figure I-4 and Figure AP-1). For calculation of the in vivo CL_{int} values, the following R_b, plasma protein binding, and $f_{u, mic}$ values were incorporated. The R_b values for gemfibrozil, mycophenolic acid, raloxifene, and biochanin A were 0.56, 0.63, 1.07, and 0.75, respectively. The plasma protein binding values for these compounds were 98.9, 99.2, 99.4, and 98.8%, respectively. The $f_{u, mic}$ values for these compounds were 0.907, 0.776, 0.278, and 0.600,

respectively. The IVIVC from intravenous clearance values was relatively good, but the $CL_{int, h}$ values of raloxifene and biochanin A obtained from the oral pharmacokinetic data were significantly underestimated, supporting the contribution of intestinal metabolism to a first-pass effect. Fa·Fg and Fh of biochanin A, mycophenolic acid, and gemfibrozil were examined after oral administration to SD rats (Table I-4). Biochanin A, which is susceptible to extremely high glucuronidation, exhibited low Fa·Fg (0.15), whereas gemfibrozil and mycophenolic acid, compounds with relatively low CL_{int} for glucuronidation, demonstrated high Fa·Fg (1.40 and 1.17, respectively).

I-iv. Discussion

Conjugation reactions have been increasingly recognized as important metabolic processes that play a strong role in the pharmacokinetics of some drugs; therefore, prediction of the clearance of such drugs is necessary. However, unlike that for P450 substrates, the IVIVC for UGT substrates has not been studied adequately because the amount of UGTs expressed in tissues is uncertain, and the intraluminal localization of the catalytic sites, which require activation for in vitro glucuronidation, makes IVIVC more complex (Lin and Wong, 2002). UGTs are widely expressed in various tissues including the liver, kidney, and gastrointestinal tract (Ohno and Nakajin, 2009), and the importance of extrahepatic glucuronidation has been reported (Ritter et al., 2007). Flavonoids (polyphenolic phytochemicals) were used as model UGT substrates in several studies in which not only hepatic but also intestinal glucuronidation and subsequent excretion by efflux transporters were reported (Jia et al., 2004; Zhang et al., 2007).

Raloxifene also has phenolic groups, and its oral bioavailability in humans is very low because of a high glucuronidation rate catalyzed by UGT1A8 and 1A10 in the intestine (Kemp et al., 2002; Jeong et al., 2005; Mizuma, 2009); its conjugates are subsequently excreted into the gut lumen by P-glycoprotein and/or MRPs. These enzyme and transporter couplings are thought to result in long half-lives because of enteric recycling despite the extensively high oral clearance (Jeong et al., 2004; Xu et al., 2009).

In the present study, species differences in $CL_{int, u}$ for in vitro glucuronidation of raloxifene were investigated (Table I-1), and the results were compared with its pharmacokinetics (Table I-2). To activate UGT, alamethicin was used as a pore-forming agent according to previous reports (Dalvie et al., 2008; Cubitt et al., 2009). The results were consistent with those reported by others, for which the glucuronidation rates with rat or human intestinal microsomes were higher than those with rat or human liver microsomes. Our study also showed that all the $CL_{int, u}$ values among investigated animals were higher for glucuronidation than for P450 metabolism in intestinal microsomes. The

$CL_{int, u}$ values obtained with dog liver or intestinal microsomes were comparable to those with rat liver or intestinal microsomes. Comparing these in vitro $CL_{int, u}$ values with the $Fa \cdot Fg$ and Fh values in the two animals demonstrated a reasonable relationship. In humans and monkeys, the raloxifene concentrations in portal plasma were not available; therefore, $Fa \cdot Fg$ was calculated from intravenous and oral pharmacokinetic data (total clearance in human = $0.647 \, l \cdot h^{-1} \cdot kg^{-1}$; Eli Lilly clinical data) by assuming $Fh = 1 - CL_b/Q_h$ and $Fa \cdot Fg = F/Fh$. When Q_h values in humans and monkeys were set at 20.7 and 43.6 $ml \cdot min^{-1} \cdot kg^{-1}$ (Davies and Morris, 1993), the calculated $Fa \cdot Fg$ values were 0.045 and 0.041, respectively. The Fa of raloxifene in humans was reported as 0.63 (Eli Lilly clinical data), and its permeability was high in our in-house study using Caco-2 cells (data not shown). Therefore, intestinal glucuronidation must be a main factor contributing to the first-pass effect.

In the present study using Gunn and Wistar rats, it was suggested that raloxifene was glucuronidated mainly by UGT1As and to lesser extent by UGT2Bs (Figure I-3, B and D; Table I-2) because Gunn rat inherently lacks all glucuronidation activities catalyzed by the UGT1 isoforms due to mutation in exons II, commonly used region for the these isoforms (Emi, 2002). The $Fa \cdot Fg$ and Fh values in Gunn rats were 2-fold higher than those in Wistar rats, respectively, indicating that raloxifene was glucuronidated in the intestine as well as in the liver. In the comparison of EHBRs with SD rats (Figure I-3, A and C), the differences in $Fa \cdot Fg$ and Fh were small, and the ratio of glucuronides to unchanged drug in systemic plasma was much higher in EHBRs, suggesting that the excretion of raloxifene glucuronides was influenced by Mrp2. Some groups have reported a compensatory induction of enzymes and transporters in Gunn and Mrp2-deficient TR⁻ rats (Kim et al., 2003; Wang et al., 2009). Flavonoids such as apigenin are efficiently metabolized by Gunn rats because of compensatory induction of intestinal UGT 2Bs and hepatic efflux transporters, which limits their oral bioavailabilities. In our studies, $CL_{int, u}$ values for P450 metabolism determined with liver microsomes from Gunn rats and EHBRs were lower than those from Wistar and SD rats (Figure I-2); therefore, P450s responsible for the oxidation of raloxifene did not show compensatory induction.

$CL_{int, u}$ values for glucuronidation determined with microsomes from Gunn rats were lower than those from Wistar rats; implying that UGTs responsible for glucuronidation of raloxifene were not induced. Of interest, species differences in the ratio of glucuronides to unchanged drugs were observed despite comparable $CL_{int, u}$ values for glucuronidation in dogs, rats, and monkeys. These ratios in the systemic plasma in dogs, SD rats, and monkeys were 1.34 to 1.84, 9.67, and 85.0, respectively, and the ratio in humans was reported as 70 to 90 (Eli Lilly clinical data). The ratios in monkeys and humans were closer to those in EHBRs than to those in wild-type SD rats, indicating that hepatic uptake of raloxifene glucuronides into the liver and excretion of them into intestinal lumen and bile may significantly differ among these species. Expression of Mrp2/MRP2 in rat, dog, and human intestine has been reported (Mottino et al., 2000; Conrad et al., 2001), but species differences in transport activity of raloxifene glucuronides have not been reported. A schematic representation of the intestinal and hepatic disposition of raloxifene is presented in Figure I-5. Further studies are needed to understand the differences in raloxifene glucuronide levels in circulation after administration in these species.

The in vitro hepatic $CL_{int, u}$ values of raloxifene, biochanin A, mycophenolic acid, and gemfibrozil (Table I-3) for glucuronidation were scaled to whole-body clearances (milligrams per minute per kilogram body weight) and compared with their observed in vivo CL_{int} values (Figure I-4; Table I-4). These compounds have been reported to be mainly excreted in bile as glucuronides in rats (Curtis et al., 1985; Jia et al., 2004; Takekuma et al., 2007). Therefore, their total clearance values were assumed to be nearly equal to their hepatic clearance values. $CL_{int, h}$ values could be predicted quite well from the in vitro hepatic $CL_{int, u}$ values for glucuronidation except for raloxifene. The $CL_{int, u}$ value of raloxifene with rat liver microsomes in the presence of NADPH was comparable to that in the presence of UDPGA; this underestimation may be caused by the exploration that did not incorporate P450-catalyzed metabolism into hepatic clearance. The oral clearance values for raloxifene and biochanin A were much higher than the predicted values, implying that intestinal

glucuronidation was a great contributor. The in vitro intestinal $CL_{int,\,u}$ values for glucuronidation relatively corresponded to the Fa·Fg values for the four compounds investigated. Biochanin A is also a human UGT1A10 substrate, which is considered to be an important isoform in the gastrointestinal tract (Lewinsky et al., 2005). With regard to this compound, much less is known about the intestinal effect on presystemic elimination in humans and the responsible UGT isoforms in rats. There are several publications on IVIVC for UGT substrates (Kilford et al., 2009; Miners et al., 2010). It is well known that in vitro predictability of CL_{int} depends on enzyme sources, experimental conditions, and the occurrence of atypical glucuronidation kinetics. In some cases, in vitro CL_{int} values using microsomes were underestimated in comparison with in vivo values. It was reported that addition of BSA to the incubation improved the predictability from microsomal data, in particular for UGT2B7 substrates (Rowland et al., 2007, 2008). However, Kilford et al. (2009) reported that the human CL_{int} value of gemfibrozil, a UGT 2B7 substrate, was overestimated 10-fold when BSA was added to the microsomal incubation. In the present study, the rat CL_{int} value of gemfibrozil was successfully predicted using rat liver microsomes in the absence of BSA. Rat UGT isoforms responsible for glucuronidating gemfibrozil and their selectivity of substrates have not been fully elucidated; therefore, further studies are needed using recombinant UGT isozymes or specific antibodies. β-glucuronidase activity also influences on glucronidation rate in in vitro experiment. Oleson reported (2008) that typical inhibitor saccharolactone had minor effect on hydrolysis rate of glucuronides and inhibitory effect on glucuronidation rate at high concentration, therefore experimental condition should be cautiously considered if β-glucuronidase inhibitors are used. In several studies, models for Fg prediction of drugs, particularly for CYP3A substrates, which are metabolized in the small intestine, have been proposed (Galetin and Houston, 2006; Yang et al., 2007; Gertz et al., 2010; Kadono et al., 2010). These approaches were recently applied to UGT substrates (Nakamori, 2012; Wu, 2013). In the present study, Fg for four compounds estimated from in vitro intestinal CL_{int} values by Q_{gut} model (Yang, 2007) correlated well with observed Fa·Fg (Figure AP-2). These findings

indicate that evaluation of intestinal glucuronidation using microsomes is useful for determination of intestinal availability.

In most pharmaceutical companies, NCEs not susceptible to P450-catalyzed metabolism have been eagerly investigated and synthesized by introducing hydrophilic groups into their structures. Therefore, prediction of Fg for such compounds, which are often eliminated through phase II metabolism and subsequent excretion, is becoming essential. For anionic compounds, the interactions of conjugating enzymes with transporters have been increasingly recognized as an important process of elimination (Nies et al., 2008; Pang et al., 2009; Sun et al., 2010). Therefore, comprehensive studies including metabolism and transport are required.

I-v. Conclusion

The impact of intestinal glucuronidation on the pharmacokinetics of UGT substrates was investigated by in vitro and in vivo methods. The IVIVC of four Ugt substrates (raloxifene, biochanin A, gemfibrozil, and mycophenolic acid) in rats using data from liver microsomes and $CL_{int, iv}$ displayed a good relationship, but the $CL_{int, po}$ of raloxifene and biochanin A, which were extensively glucuronidated by intestinal microsomes, were higher than the predicted values using data from only liver microsomes, indicating that intestinal metabolism may be a great contributor to the first-pass effect. The in vitro intestinal CL_{int} corresponded with Fa·Fg for four Ugt substrates examined in rats. In Gunn rats, Fa·Fg and Fh of raloxifene were twice those observed in wild-type rats, indicating that raloxifene was mainly glucuronidated by Ugt1As in both the intestine and the liver. The difference in contribution of intestinal and hepatic glucuronidation of raloxifene to the first-pass effect between rats and dogs was demonstrated. These findings suggest that the evaluation of intestinal and hepatic glucuronidation for NCEs is important to improve their pharmacokinetic profiles.
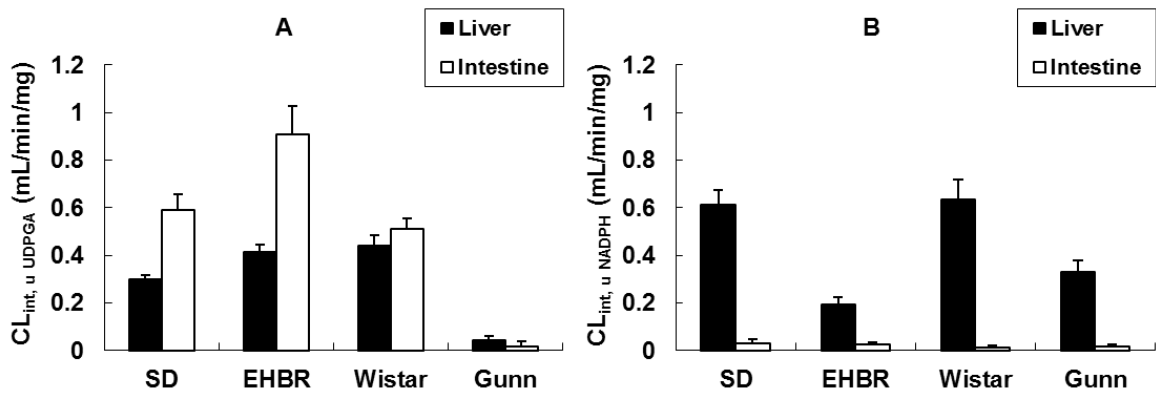
Figure I-1. The $CL_{int, u}$ of raloxifene metabolism (milliliters per minute per milligram of protein) in rat microsomes.

Microsomal incubations were fortified with A) UDPGA or B) NADPH.

■, $CL_{int, u}$ by liver; □, $CL_{int, u}$ by intestinal microsomes.

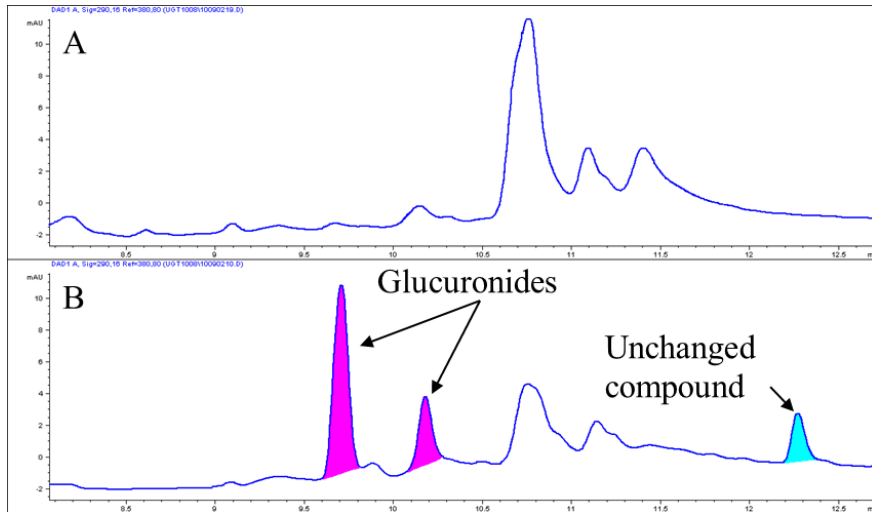Each column represents the mean and error bars indicate the S.D.

Figure I-2. HPLC chromatograms with UV detection at 290 nm of raloxifene and its metabolites.

A) rat blank plasma and B) portal plasma at 15 min after dosing raloxifene (2 mg/kg p.o.) to SD rats.
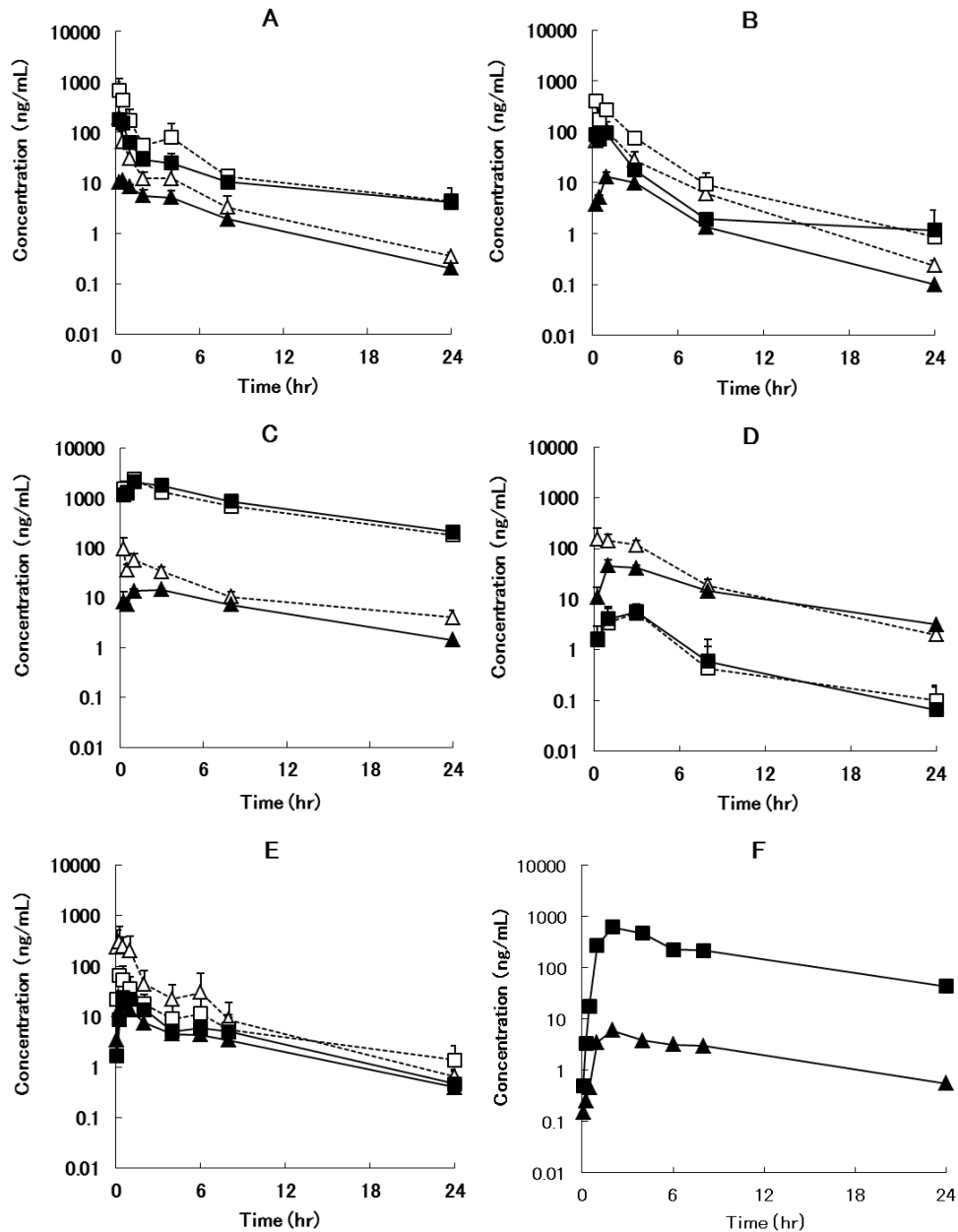
Figure I-3. Plasma concentration versus time profiles of raloxifene and its glucuronides after oral administration.

Closed symbols ■, systemic plasma concentrations; open symbols □, portal plasma concentrations.

▲ and △, raloxifene; ■ and □, glucuronides.

Raloxifene was dissolved in ethanol, polyethylene glycol 300, and water (1:4:5) and administered at 2 mg/kg to A) SD rats, B) Wistar rats, C) EHBRs, D) Gunn rats, E) beagle dogs, and F) cynomolgus monkeys. Each symbol represents the mean and the error bars indicate the S.D.
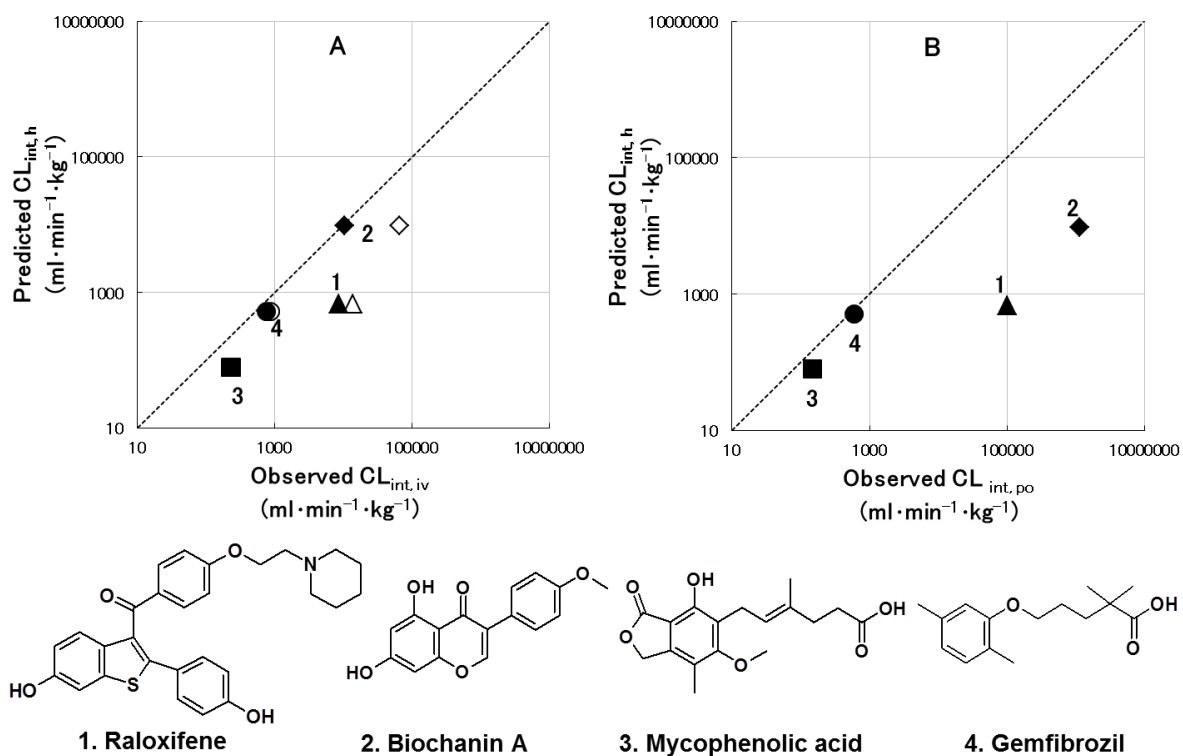
Figure I-4. Comparison of predicted and observed $CL_{int, h}$ values in SD rats.

$CL_{int, h}$ values were predicted using rat liver microsomes fortified with UDPGA. A) comparisons of predicted and observed $CL_{int, h}$ values from intravenous pharmacokinetic data obtained from the well stirred (open) and parallel tube (closed) liver models for four compounds. B) comparison of predicted and observed $CL_{int, h}$ values from oral pharmacokinetic data that assumed complete absorption and no intestinal metabolism. Dashed lines represent $Y = X$.
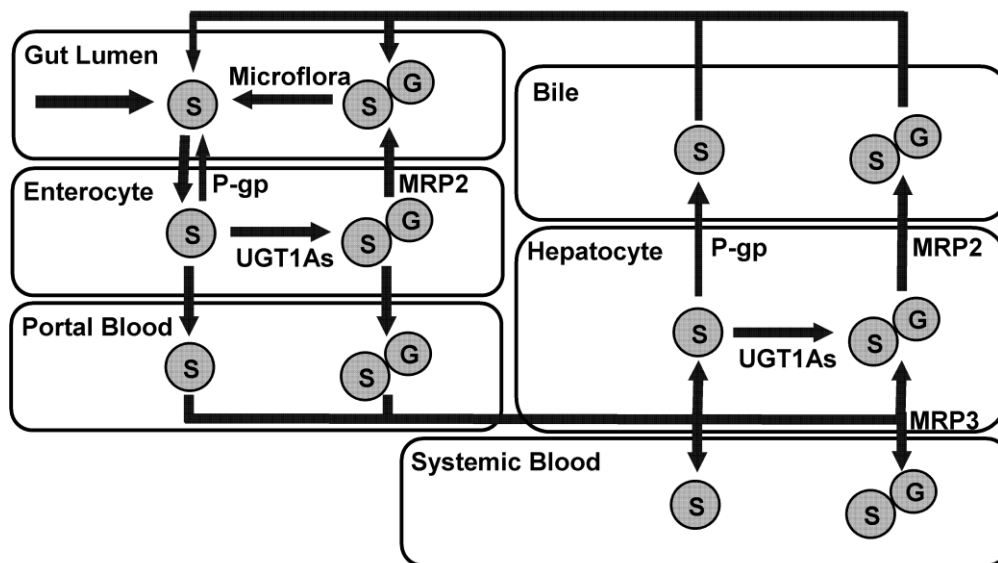
Figure I-5. Schematic representation of intestinal and hepatic disposition of raloxifene

S, raloxifene; G, glucuronic acid; P-gp, P-glycoprotein.

Table I-1. $CL_{int, u}$ of raloxifene metabolism by rat, dog, monkey, and human liver and intestinal microsomes.

Microsomes	$CL_{int, u}$			
	UGT		P450	
	Liver	Intestine	Liver	Intestine
	$ml \cdot min^{-1} \cdot mg\ protein^{-1}$			
Rat	0.359 ± 0.038	0.992 ± 0.099	0.293 ± 0.096	0.019 ± 0.007
Dog	0.693 ± 0.086	1.344 ± 0.088	0.884 ± 0.033	0.092 ± 0.012
Monkey	0.289 ± 0.075	1.737 ± 0.692	0.386 ± 0.027	0.375 ± 0.009
Human	0.470 ± 0.051	3.284 ± 0.268	0.119 ± 0.022	0.028 ± 0.008

Microsomal incubations were fortified with UDPGA or NADPH. $CL_{int, u}$ values represent the mean ± S.D. of three determinations.

Table I-2. Pharmacokinetic parameters of raloxifene after intravenous or oral administration to SD rats, EHBRs, Wistar rats, Gunn rats, beagle dogs, and cynomolgus monkeys

Animals	1 mg/kg i.v.			2 mg/kg p.o.						
	CL_{tot}	Vd_{ss}	AUC	C_{max}	AUC	Glu/Parent ratio		F_h	$F_a \cdot F_g$	F
						Portal	Systemic			
	$ml \cdot h^{-1} \cdot kg^{-1}$	ml/kg	$ng \cdot h/ml$	ng/ml	$ng \cdot h/ml$					
SD rats	2051 (172)	3240 (440)	490 (42)	11.4 (0.7)	58.3 (15.2)	5.73 (1.14)	9.67 (4.65)	0.33 (0.11)	0.16 (0.08)	0.048 (0.014)
EHBRs	1323 (153)	3673 (499)	762 (84)	14.5	160	46.8	129	0.43	0.26	0.11
Wistar rats	1475 (323)	4015 (1673)	704 (176)	13.0	68.2	2.51	3.80	0.20	0.34	0.067
Gunn rats	1305 (158)	4967 (595)	775 (100)	45.2	389	0.03	0.09	0.43	0.63	0.27
Dogs										
Intact	1057	3157	976	16.0 (2.3)	85.7 (15.6)	N.D.	1.84 (0.61)	N.D.	N.D.	0.044 (0.008)
Cannulated	1163	3022	860	23.3 (1.4)	87.4 (20.9)	0.27 (0.10)	1.34 (0.52)	0.16 (0.04)	0.36 (0.18)	0.052 (0.014)
Monkeys	909	3847	1102	6.0	62.2	N.D.	84.98	N.D.	N.D.	0.026

N.D., not determined.

If AUCpv was not available (intact dogs and monkeys), F was calculated by dividing the oral AUCs by the intravenous AUCs corrected for dose. Values in parentheses represent S.D.s.

Table I-3. $CL_{int, u}$ of gemfibrozil, mycophenolic acid, raloxifene, and biochanin A metabolism by rat liver and intestinal microsomes.

Microsomes	$CL_{int, u}$							
	UGT				P450			
	Liver		Intestine		Liver		Intestine	
	ml · min^{-1} · mg protein^{-1}							
Gemfibrozil	0.273	± 0.008	0.001	± 0.002	0.025	± 0.008	0.002	± 0.002
Mycophenolic acid	0.042	± 0.006	0.229	± 0.014	0.006	± 0.003	0.002	± 0.001
Raloxifene	0.359	± 0.038	0.992	± 0.099	0.293	± 0.096	0.019	± 0.007
BiochaninA	5.050	± 0.744	2.845	± 0.234	0.062	± 0.004	0.004	± 0.004

Microsomal incubations were fortified with UDPGA or NADPH. $CL_{int, u}$ values represent the mean ± S.D. of three determinations.

Table I-4. Pharmacokinetic parameters of gemfibrozil, mycophenolic acid, raloxifene, and biochanin A after intravenous or oral administration to SD rats.

Compounds	Intravenous				Oral							
	Dose	CL_{tot}	Vd_{ss}	AUC	Dose	C_{max}	AUC	Glu/Parent ratio		Fh	Fa·Fg	F
								Portal	Systemic			
	mg/kg	$ml \cdot h^{-1} \cdot kg^{-1}$	ml/kg	$ng \cdot h/ml$	mg/kg	ng/ml	$ng \cdot h/ml$					
Gemfibrozil	3	437 (154)	2234 (1397)	7626 (3244)	30	44,583 (31,358)	62,320 (20,397)	0.17 (0.03)	0.18 (0.01)	0.65 (0.16)	1.40 (0.64)	0.85 (0.19)
Mycophenolic acid	3	107 (49)	637 (265)	34,366 (20,858)	10	46,901 (2900)	135,027 (23,271)	N.D.	N.D.	0.94	1.17	1.10
Raloxifene	1	2051 (172)	3240 (440)	490 (42)	2	11.4 (0.7)	58.3 (15.2)	5.73 (1.14)	9.67 (4.65)	0.33 (0.11)	0.16 (0.08)	0.048 (0.014)
Biochanin A	5	3228 (527)	938 (465)	1578 (265)	50	6.0 (2.2)	69.9 (34.4)	2.98 (0.99)	110 (73)	0.016 (0.008)	0.15 (0.06)	0.0024 (0.0012)

N.D., not determined.

Values in parentheses represent S.D.s. For mycophenolic acid, the S.D. was not calculated because the difference between systemic and portal AUCs was too small; therefore, Fa·Fg was estimated from each averaged AUC.

31

Chapter II

Hepatic uptake and biliary excretion of raloxifene glucuronide and the other compounds

II-i. Introduction

In the chapter I, we observed that the blood concentration ratio of raloxifene glucuronides to the parent drug was greater in EHBRs (129) than that in SD rats (10). The blood concentration ratio of raloxifene glucuronides to the parent drug in humans is as high as 70–90 (Eli Lilly clinical data), a value similar to that in EHBRs. The glucuronidation activities of the liver and intestinal microsomes for raloxifen were comparable between these two rat strains, suggesting that an alteration of metabolism could not explain the difference in glucuronide exposure between SD rats and EHBRs (Kosaka et al., 2011). The simplest interpretation is that raloxifen glucuronides are transport substrates of Mrp2 and that its genetic deficiency in EHBR results in the accumulation of these conjugates in hepatocytes that then flow back into the blood. In line with this interpretation, the expression of MRP2 in normal human liver is considerably lower than that in SD rat liver (Ninomiya et al., 2005; Li et al., 2009). However, secondary alteration in sinusoidal transporters expression and/or the inhibition of their function by endogenous substances such as bilirubin glucuronides (Mrp2 substrate, Cui et al., 2001), possibly exaggerate the phenotypic differences between SD rats and EHBRs or between experimental animals and humans. The induction of Mrp3 (a sinusoidal efflux transporter of organic anions) and down-regulation of Oatp1a1 and Oatp1a4 (sinusoidal uptake transporters of organic anions) are observed in EHBRs (Kuroda et al., 2004). Moreover, MRP3 is highly expressed in the normal state in human liver (Ohtsuki et al., 2012; Chu et al., 2013), so that it is important to determine whether the phenotypic difference observed in EHBR is attributable solely to Mrp2 deficiency or also to other effects. Such generic interpretation, not restricted to Mrp2/MRP2, would improve the predictability of the in vivo disposition of organic anions in humans based on that in rats.

In the present study, we focused particularly on the pharmacokinetic differences of organic anions including R6G between SD rats and EHBRs to determine whether they could be explained solely by a difference in its biliary excretion process, and conducted further investigation into a hepatic uptake process.

II-ii. Materials and Methods

Reagents. [^{14}C]raloxifene (59 mCi/mmol, 99%) was purchased from Perkin Elmer (Boston, MA). Raloxifene-6-glucuronide (R6G) was obtained from Toronto Research Chemicals (Toronto, Canada). Non-labeled estradiol-17β-glucuronide (E$_2$17βG) and [^{3}H] E$_2$17βG (34 Ci/mmol, 97%) were purchased from Sigma-Aldrich and Perkin Elmer, respectively. valsartan was obtained from Wako (Osaka, Japan). Human intestinal microsomes were obtained from XenoTech, LLC (Lenexa, KS). The UGT reaction mix solution (250 mM Tris-HCl, 40 mM MgCl$_2$, and 0.125 mg/ml alamethicin) was purchased from BD Gentest (Woburn, MA). Rat Mrp2 and control vesicle (insect Sf9 cells/baculovirus systems expressing transporters) and a vesicular transport assay reagent kit were purchased from Geno Membrane (Kanagawa, Japan). All chemicals were of analytical grade or the highest quality available.

Animals. All animal procedures were conducted under protocols approved by the Mitsubishi Tanabe Institutional Animal Care and Use Committee. Male SD rats and EHBRs 7 to 8 weeks old were obtained from Japan SLC (Shizuoka, Japan).

Synthesis of [^{14}C]R6G. [^{14}C]Raloxifene was glucuronidated using human intestinal microsomes fortified with UDPGA (a UGT reaction mix solution). The resulting [^{14}C] R6G was purified by high-pressure liquid chromatography (HP1100 system; Agilent Technologies, Santa Clara, CA) on a column (Symmetry C18; 3.5 μm particle size, 4.6 mm i.d. × 150 mm, Waters) with isocratic elution using acetonitrile and 10 mM ammonium acetate and desalted with salt-free mobile phase. [^{14}C] R6G was identified by comparison with unlabeled synthetic standards using a liquid chromatography–mass spectrometer/mass spectrometer (LC-MS/MS) system (Quattro Micro, Waters, Milford, MA).

Vesicular Transport Assays. The time- and concentration-dependent transport of [^{14}C] R6G into rat Mrp2-expressing membrane vesicles and control membrane vesicles (insect Sf9 cells/baculovirus systems) was investigated according to the manufacturer's instructions (Geno Membrane) using the

rapid filtration technique. In brief, the transport medium (final, 10 mM MOPS-Tris, 14 mM KCl, 4 mM MgATP (or MgAMP) and 2 mM GSH, pH 7.4) containing R6G (time-dependent transport, 0.625μM; concentration-dependent transport, 0.625, 1.25, 2.5, 5, 7.5, 12.5, 25, 37.5, and 50 μM) was mixed with the vesicle suspension. At a designated time (time-dependent transport, 1, 3, 5, and 10 min; concentration-dependent transport, 3 min), the transport reaction was stopped by the addition of an ice-cold buffer (40 mM MOPS-Tris, 70 mM KCl, pH 7.4) and filtered (MulitiScreen, Millipore). The filters were washed with the same ice-cold buffer three times. The radioactivity retained on the filters was analyzed with a liquid scintillation counter (TRI-CARB 3100TR, Perkin Elmer). ATP-dependent uptake into vesicles was calculated by subtracting data generated with AMP from ATP data, and resulting values for control vesicles were subtracted from those for Mrp2-expressing vesicles to estimate Mrp2-specific transport.

Pharmacokinetic Studies of R6G. R6G (0.5 μmol/kg) was intravenously administered to bile duct-canulated rats (n = 3). Blood was collected at 0.05, 0.25, 0.5, 1, 2, 4, 6, 8, and 24 h after administration. Bile was accumulated at the designated time periods (0–0.25, 0.25–0.5, 0.5–1, 1–2, 2–4, 4–8, and 8–24 h) after administration. The plasma was separated from the blood by centrifugation. The plasma and bile samples were processed for analysis by protein precipitation with acetonitrile. Standard samples containing the same matrices were prepared, and the compound concentrations were quantified by LC-MS/MS. Total clearance (CL_{total}) was calculated as dose/AUC. Vd_{ss} was calculated as the product of CL_{total} and MRT obtained by moment analysis. Biliary clearance (CL_{bile}) based on plasma concentration was calculated as the product of excretion rate and CL_{total}.

Integration Plot Studies in the Rat Liver. Three compounds (R6G, 0.1 μmol/kg; valsartan, 0.5 μmol/kg; $E_2$17βG, 0.5 μmol/kg) were intravenously administered to rats (n = 3) each. Blood was collected at 1 min, 3 min, and 5 min after administration and the liver was isolated at the final point. The plasma was separated from the blood by centrifugation. The liver was homogenized with saline and acetonitrile and centrifuged, and the protein precipitate was removed. Standard samples

containing the same matrices were prepared, and the compound concentrations were quantified by LC-MS/MS. Hepatic uptake clearance was calculated from the slope of an integration plot.

Compartmental Pharmacokinetic Modeling of R6G Disposition in Rats in vivo. Compartmental pharmacokinetic modeling was performed using NAPP version 2.31 software (Hisaka and Sugiyama 1998). Five kinetic parameters, including the volume of distribution (S1), elimination rate constant (k_e), hepatic uptake rate constant (k_{12}), sinusoidal efflux rate constant (k_{21}), and biliary excretion rate constant (k_{bile}), were estimated (Figure II-1). In this model, R6G is assumed to distribute mainly in liver as a peripheral compartment. Although a peripheral compartment may be influenced by an extra-hepatic organ, it was excluded because separation of hepatic and extra-hepatic compartments was difficult.

Statistics. Data were analyzed using Microsoft Excel 2010. Statistical significances were tested by the two-tailed Student's *t* test. Probability (P) values are symbolized by: $* = P < 0.05$, $** = P < 0.01$, and $*** = P < 0.001$. $P < 0.05$ was considered statistically significant.

II-iii. Results

Vesicular Transport Assays. The transport of [^{14}C] R6G was evaluated using rat Mrp2 expressing-membrane vesicles. ATP-dependent uptake was enhanced in Mrp2-expressing vesicles as compared to the control vesicles (Figure II-2A). ATP-dependent uptake into Mrp2-expressing vesicles was time-dependent. Uptake was linear during at least the initial 5 min. The concentration dependence of the initial 5-min uptake was evaluated and Mrp2-dependent uptake was calculated by a subtraction of the uptake into control vesicles (possibly mediated by endogenous transporters expressed in Sf9 cells) from that into Mrp2-expressing vesicles in the presence of ATP, and plotted as an Eadie–Hofstee plot (Figure II-2B). The uptake of [^{14}C] R6G by rat Mrp2-expressing membrane vesicles exhibited a two-phase kinetic profile. The higher-affinity Km of 1.9 μM was obtained, but the lower component was not calculated, at least under our experimental conditions (R6G concentration range of 0.625–50 μM). Uptake of [^{14}C] R4'G, major metabolite of raloxifene in human, into human MRP2- and MRP3-expressing membrane vesicles was also enhanced in the presence of ATP (Figure AP-4).

In vivo Disposition of R6G in SD rats and EHBRs. Concentrations of R6G in plasma and bile after the intravenous administration of R6G (0.5 μmol/kg) to bile duct-canulated SD rats and EHBRs showed clear differences from each other (Figure II-3). The model-independent parameters are shown in Table II-1. CL$_{total}$ and biliary efflux clearance (CL$_{bile}$) of R6G based on plasma concentration were significantly decreased in EHBR as compared to that in SD rats. These findings are consistent with the function of R6G as a transport substrate of Mrp2 (Figure II-2).

Compartmental Pharmacokinetic Modeling of R6G Disposition in Rats in vivo. Time profiles of R6G plasma concentration and R6G cumulative biliary amounts in rats were fitted to the two-compartment model shown in Figure II-1. As a result, significant decreases not only in biliary excretion, which are likely to be attributable to the Mrp2-mediated transport process (k$_{bile}$), but also in the hepatic uptake process (k$_{12}$) were observed in EHBRs (Table II-2). To ascertain whether the reduction in hepatic uptake generally occurs in EHBRs, two-compartment models for the other Mrp2

37

substrates valsartan and E$_2$17βG were fitted, using literature data reported by Yamashiro (2006) and Morikawa (2000), respectively. Thus, the hepatic uptake of valsartan was much lower in EHBRs than that in SD rats. In contrast, the hepatic uptake of E$_2$17βG was comparable between SD rats and EHBRs (Table AP-1 and Figure AP-3).

Integration Plot Studies in the Rat Liver. An integration plot study of R6G (0.1 μmol/kg) in the liver was conducted in SD rats and EHBRs. As expected from the data in pharmacokinetic modeling, hepatic uptake clearance of R6G was significantly lower (with a 66% reduction) in EHBRs than that in SD rats (Figure II-4A and Table II-3). This result indicated that Mrp2 deficiency collaterally attenuated the hepatic uptake of R6G. Moreover, integration plot studies of valsartan (0.5 μmol/kg) and E$_2$17βG (0.5 μmol/kg) were conducted. As a result, the hepatic uptake clearance of valsartan was lower (with a 95% reduction) in EHBRs than that in SD rats, whereas the hepatic uptake clearance of E$_2$17βG was similar between the rat strains (Figure II-4B, 4C and Table II-3).

II-iv. Discussion

In the present study, we confirmed that biliary excretion of R6G is mediated by Mrp2 through the three experiments: 1) uptake into Mrp2-expressing membrane vesicles (Figure II-2), 2) compartmental pharmacokinetic modeling after bolus injection (Figure II-3 and Table II-2), and 3) biliary clearance under steady state after intravenous infusion (Figure AP-5 and Table AP-2). In the analysis of compartmental pharmacokinetic modeling of R6G, we unexpectedly observed that the hepatic uptake rate constant (k_{12}) was significantly reduced in EHBRs as compared to SD rats in addition to the reduction in the biliary excretion rate constant (k_{bile}). The reduction in hepatic uptake clearance of R6G in EHBRs was confirmed by the integration plot analysis (Figure II-4A and Table II-3). To ascertain whether the reductions in hepatic uptake generally occur in EHBRs, literature data of organic anions including plasma and bile concentration in SD rats and EHBRs were collected and classified based on the difference in initial distribution between these rats (Table AP-3). The pharmacokinetics of valsartan in SD rats and EHBRs were reported by Yamashiro et al. (2006). Our analysis by the two-compartment modeling for valsartan using their data suggested that not only k_{bile} but also the k_{12} were much reduced in EHBRs as compared to those in SD rats (Table AP-1 and Figure AP-3A, B). This finding is consistent with the results of our integration plot analysis (Figure II-4B and Table II-3). The pharmacokinetics of $E_217\beta G$ after intravenous administration in SD rats and EHBRs were reported at the tracer level (Morikawa et al., 2000). As shown in Table AP-1 and Figure AP-3C and D, our analysis by the two-compartment modeling for $E_217\beta G$ using their data indicated that k_{12} values were comparable between SD rats and EHBRs. It is also accordant with the result of integration plot analysis shown in this study (Figure II-4C and Table II-3). The plasma concentrations at 1 min in SD rats and EHBRs in integration plot studies were as follows: R6G, 0.88 ± 0.09 μM and 1.44 ± 0.25 μM; valsartan, 8.1 ± 0.4 μM and 11.5 ± 0.6 μM; $E_217\beta G$, 2.9 ± 0.5 μM and 3.7 ± 1.0 μM, respectively. The liver concentrations at 1 min in SD rats and EHBRs in these studies were as follows: R6G, 0.59 ± 0.10 μM and 0.47 ± 0.13 μM; valsartan, 5.4 ± 0.9 μM and 0.85 ± 0.28 μM; $E_217\beta G$, 8.3

± 0.8 μM and 4.6 ± 1.0 μM, respectively. The free fraction of R6G in SD rat and EHBR plasma were 0.038 ± 0.011 and 0.042 ± 0.009, respectively. The free fraction of R6G in SD rat and EHBR liver were 0.051 ± 0.004 and 0.058 ± 0.011, respectively. Comparable plasma concentrations between these rats imply that the saturation in hepatic uptake did not occur in EHBRs, even if free fraction of the compound concentration is not taken into consideration. However further examination of dose dependency is needed to exclude the possibility of the saturation in hepatic uptake of these compounds. It is known that $E_2 17\beta G$ is transported by Oatp1a1, Oatp1a4, and Oatp1b2 on the sinusoidal membrane of hepatocytes in rats, and the Km values have been reported to be 3–20, 3, and 32 μM, respectively (Hagenbuch et al., 2003). The reason why the hepatic uptake of organic anions is decreased for some compounds but not for others in EHBR is unclear at present. One reason for the difference may be that the substrate specificities of these transporters overlap to some extent but are not identical, and that expression and/or function of those are differentially affected in EHBR. Kuroda et al. (2004) reported that the hepatic expression of Mrp3 was induced and those of Oatp1a1 and Oatp1a4 protein were reduced adaptively in EHBRs by a compensatory mechanism for mitigating injury to hepatocytes from cytotoxic materials that increase in Mrp2 deficiency. In our preliminary study, the in vitro uptake into freshly isolated hepatocytes from SD rats and EHBRs exhibited no difference for any of the compounds tested (Figure AP-6 and 7). The discrepancy between the in vivo and in vitro results may have been due to the suppression of transporter function and/or expression during the isolation of hepatocytes from SD rats. Lundquist et al. recently reported (2014a, b) the impact of transporter loss in human and rat cryopreserved hepatocytes on clearance predictions. They found that rat Oatp2b1 protein was significantly reduced after cell isolation and further after cryopreservation, compared with liver tissue. In their study, the hepatic uptake clearance was somewhat underestimated when fresh hepatocytes were used. In addition to the down-regulation of the amount of transporters in the cells, internalization of the transporters from the cell surface is also possible. It has been reported that human OATP2B1 and OATP1B3 are rapidly internalized by the

protein kinase C activator, phorbol- 12-myristate-13-acetate (PMA) (Köck et al, 2010; Powell et al, 2014). This possibility remains to be elucidated in future. Another hypothesis explaining the difference in pharmacokinetics between SD rats and EHBRs is the inhibition of the transport function by endogenous substances such as bilirubin glucuronides. Bilirubin glucuronide (direct bilirubin) concentration in plasma was reported to be as high as 49.1 μM in EHBR, whereas that in SD rat was only 1.05 μM (Sathirakul et al., 1993). It has been reported that rat Oatp1a1 accepts bilirubin monoglucuronide as a transport substrate, but rat Oatp1a4 does not (Reichel et al., 1999), and that the Km values for human OATP1B1 and OATP1B3 were 0.10 and 0.50 μM, respectively (Cui et al., 2001). We preliminarily tested this hypothesis by comparing the effects of SD rat plasma and EHBR plasma (50% and 95%, each) on the transport of [^{14}C]R6G into isolated hepatocytes prepared from SD rats (Figure AP-8). Both plasma similarly reduced the uptake of [^{14}C]R6G into hepatocytes and showed no differences, at least under our experimental conditions. The effect independent of the plasma of rat strains is likely attributable to a decrease in the unbound concentration of [^{14}C]R6G in the presence of plasma protein. The binding of R6G to plasma protein in both rat strains is so high as described above, that reduction of the unbound concentration of R6G in the transport medium obscured the inhibitory effect of bilirubin glucuronide in EHBR plasma on the uptake of R6G into hepatocytes. An understanding of the mechanism explaining the difference in hepatic uptakes of organic anions between SD rats and EHBRs awaits further investigation.

II-v. Conclusion

The hepatic uptake and biliary excretion process of organic anions in SD rats and EHBRs were investigated. R6G was confirmed to be a substrate of MRP2/Mrp2 by in vitro and in vivo methods. Pharmacokinetic modeling of R6G indicated that reduction in not only biliary excretion but also hepatic uptake of R6G influenced to low plasma clearance in EHBRs compared to SD rats. The reduction in hepatic uptake of R6G in EHBRs was confirmed by integration plot study. The reduction was also observed for valsartan but not for $E_2 17\beta G$. This variation may be related to the difference in substrate specificity of organic anion transporters and/or inhibition of hepatic uptake by endogenous substances such as bilirubin glucuronides. Incidental alteration of hepatic uptake for organic anions should be considered to explain their enhanced systemic exposure in EHBRs. This finding is important for a better prediction of the drug disposition in humans based on animal or in vitro uptake experiments.
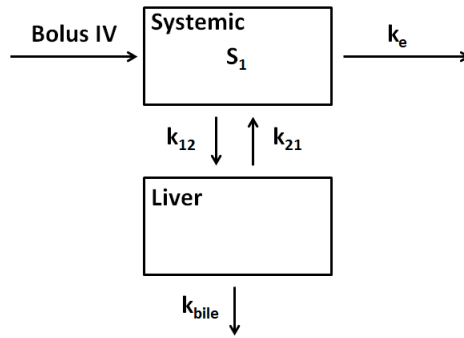
Figure II-1. Compartmental pharmacokinetic modeling

S_1, k_e, k_{12}, k_{21}, and k_{bile} represent the volume of distribution, elimination rate constant, hepatic uptake rate constant, sinusoidal rate efflux constant, and biliary excretion rate constant, respectively.
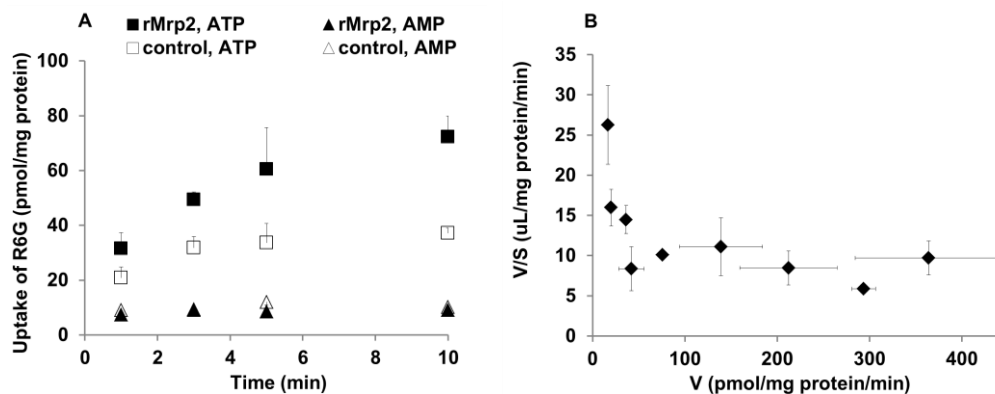
Figure II-2. Time- and concentration-dependent transport of [^{14}C] R6G into rat Mrp2-expressing membrane vesicles.

A) Time-dependent uptake of [^{14}C] R6G into rat Mrp2-expressing membrane vesicles and control membrane vesicles in the presence of ATP/AMP. Closed and open symbols represent rat Mrp2-expressing membrane vesicles and control membrane vesicles, respectively. Square and triangular symbols represent the reactions with ATP and AMP, respectively. B) Eadie–Hofstee plot of [^{14}C] R6G uptake by rat Mrp2 membrane vesicles. Mrp2-dependent uptake was calculated by a subtraction of the uptake into control vesicles from that into Mrp2-expressing vesicles.
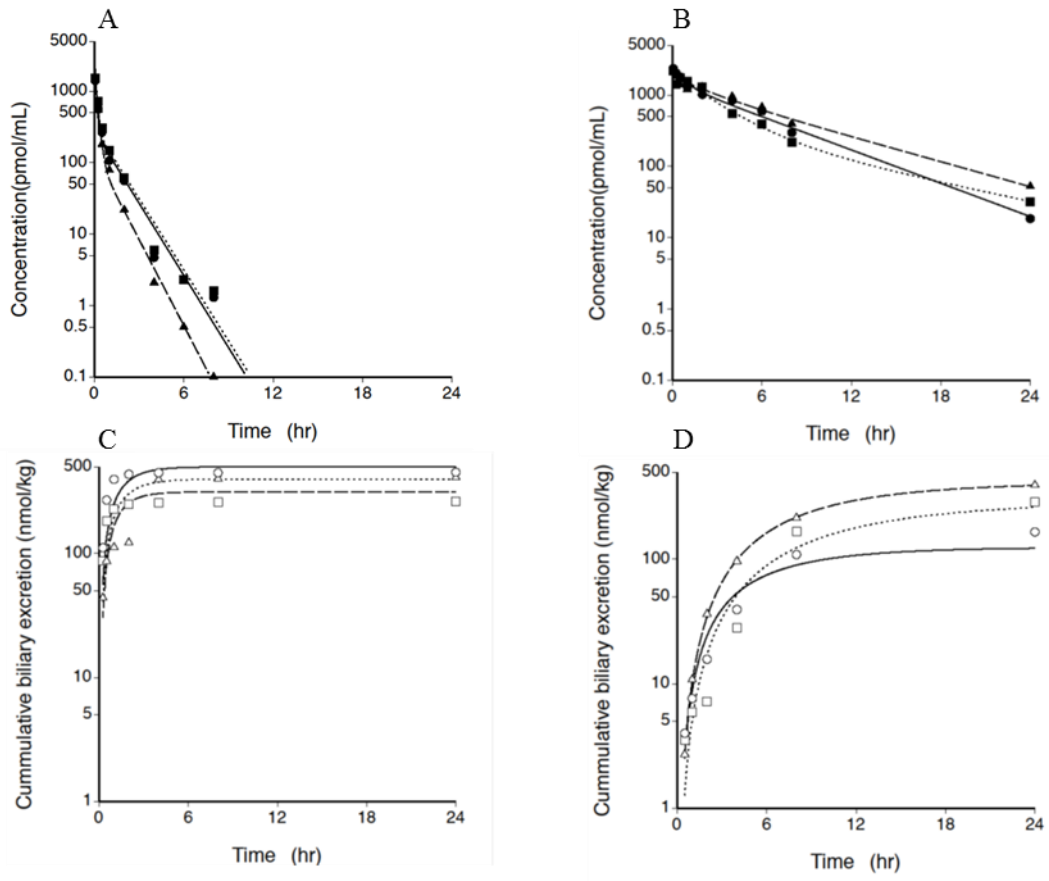
Figure II-3. Compartmental pharmacokinetic modeling of R6G after bolus injection (0.5 µmol/kg) in rats.

Individual time profiles of R6G plasma concentration in A) SD rats and B) EHBRs, and R6G cumulative biliary amounts in C) SD rats and D) EHBRs were fitted to the two-compartment model shown in Figure 1. Closed and open symbols represent plasma concentration and cumulative biliary excretion, respectively. Circular, square, and triangular symbols represent the individual values observed. Solid, dotted, and dashed lines represent the individual time-concentration curves simulated.
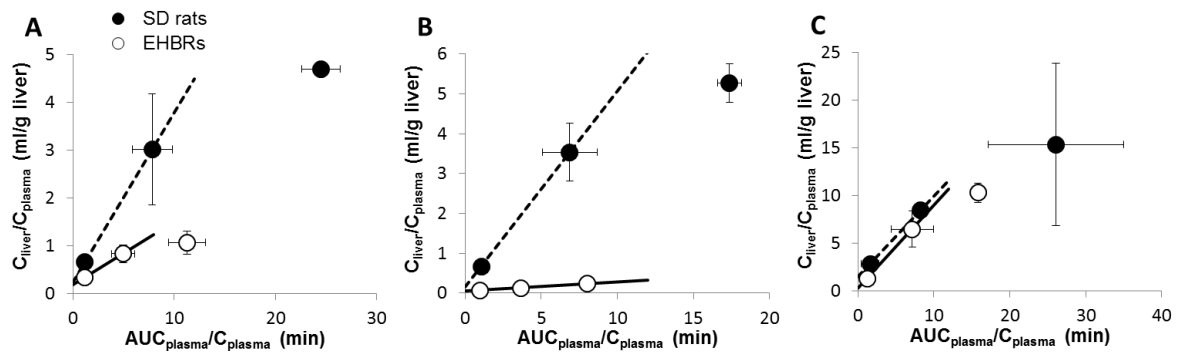
Figure II-4. Integration plots of Mrp2 substrates in the rat liver: A) R6G, B) valsartan, C) $E_2 17\beta G$

R6G (0. 1 μmol/kg), valsartan (0.5 μmol/kg), and $E_2 17\beta G$ (0.5 μmol/kg) were each intravenously administered to rats (n = 3). Blood and liver samples were collected at 1, 3 and 5 min after administration. Closed and open symbols represent the plot of SD rats and EHBRs, respectively. Slopes of integration plots represent hepatic uptake clearance.

Table II-1. Model-independent pharmacokinetic parameters after the bolus injection of R6G in SD rats and EHBRs.

	SD rats	EHBRs
CL_{tot} (*ml $\cdot min^{-1} \cdot kg^{-1}$*)	13.3 ± 2.12	0.833 ± 0.117 ***
CL_{bile} (*ml $\cdot min^{-1} \cdot kg^{-1}$*)	10.4 ± 1.47	0.425 ± 0.083 ***
Vd_{ss} (*ml/kg*)	486 ± 97	262 ± 23 *

* = P < 0.05; ** = P < 0.01; *** = P < 0.001 versus SD rats

R6G (0.5 μmol/kg) was intravenously administered to bile duct-canulated SD rats and EHBRs (n = 3). Biliary clearance (CL_{bile}) based on plasma concentration was calculated as the product of total clearance and excretion rate. Means ± standard deviations are presented.

Table II-2. Kinetic parameters of R6G after bolus injection in SD rats and EHBRs

	SD rats	EHBRs
S_1 (*l/kg*)	0.193 ± 0.036	0.243 ± 0.027
k_e (*1/h*)	0.854 ± 0.837	0.111 ± 0.083
k_{12} (*1/h*)	7.297 ± 3.068	0.267 ± 0.086 *
k_{21} (*1/h*)	0.745 ± 0.316	0.282 ± 0.352
k_{bile} (*1/h*)	0.822 ± 0.064	0.168 ± 0.078 ***

* = $P < 0.05$; ** = $P < 0.01$; *** = $P < 0.001$ versus SD rats

Time profiles of R6G plasma concentration and R6G cumulative biliary amount in rats (0.5 μmol/kg) were fitted to the two-compartment model shown in Figure II-1. Means ± standard deviations are presented.

Table II-3. Hepatic uptake clearance of Mrp2 substrates in SD rats and EHBRs in an integration plot study.

Compounds	CL_{uptake}		Reduction rate in EHBRs compared with SD rats
	SD rats	EHBRs	
	$ml \cdot min^{-1} \cdot g \; liver^{-1}$		
R6G	0.394 ± 0.086	0.135 ± 0.031 **	66%
valsartan	0.465 ± 0.104	0.024 ± 0.004 ***	95%
$E_2 17\beta G$	0.856 ± 0.055	0.798 ± 0.189	no change

* = $P < 0.05$; ** = $P < 0.01$; *** = $P < 0.001$ versus SD rats

R6G (0.1 μmol/kg), valsartan (0.5 μmol/kg), and $E_2 17\beta G$ (0.5 μmol/kg) were intravenously administered to the rats (n = 3) each. Blood and liver samples were collected at 1, 3 and 5 min after administration. Uptake clearance was calculated from the slope of an integration plot. Means ± standard errors are presented.

Conclusion

In the chapter I, this study demonstrated that 1) the intestinal glucuronidation of raloxifene and biochanin A effectively lower the bioavailability, 2) Ugt1As play a major role in the glucuronidation of raloxifene in both liver and intestine, and 3) there is a species difference in contribution of intestinal and hepatic glucuronidation of raloxifene to the first-pass effect between rats and dogs. These findings suggest that the evaluation of intestinal and hepatic glucuronidation for NCEs is important to improve their pharmacokinetic profiles.

In the chapter II, this study demonstrated that the hepatic uptakes for R6G and valsartan were reduced in EHBRs compared to SD rats, but not for $E_2 17\beta G$. This mechanism is unclear at present. It may be related to the difference in substrate specificity of transporters and/or inhibition of hepatic uptake by endogenous substances. It is desirable to consider the possibility of secondary effects on the hepatic uptake process for organic anions to explain their enhanced systemic exposure in EHBRs. This finding is important for a better prediction of the drug disposition in humans based on animal or in vitro uptake experiments.

References

Conrad S, Viertelhaus A, Orzechowski A, Hoogstraate J, Gjellan K, Schrenk D, and Kauffmann HM (2001) Sequencing and tissue distribution of the canine MRP2 gene compared with MRP1 and MDR1. *Toxicology* **156:**81–91.

Chu X, Bleasby K, Evers R (2013) Species differences in drug transporters and implications for translating preclinical findings to humans. *Expert Opin Drug Metab Toxicol* **9**:237–52.

Cubitt HE, Houston JB, and Galetin A (2009) Relative importance of intestinal and hepatic glucuronidation-impact on the prediction of drug clearance. *Pharm Res* **26:**1073–83.

Cui Y, König J, Leier I, Buchholz U, Keppler D (2001) Hepatic uptake of bilirubin and its conjugates by the human organic anion transporter SLC21A6. *J Biol Chem* **276**:9626–30.

Curtis CG, Danaher TM, Hibbert EA, Morris CL, Scott AM, Woolcott BA, and Powell GM (1985) The fate of gemfibrozil and its metabolites in the rat. *Biochem Soc Trans* **13:**1190–91.

Dalvie D, Kang P, Zientek M, Xiang C, Zhou S, and Obach RS (2008) Effect of intestinal glucuronidation in limiting hepatic exposure and bioactivation of raloxifene in humans and rats. *Chem Res Toxicol* **21:**2260–71.

Davies B and Morris T (1993) Physiological parameters in laboratory animals and humans. *Pharm Res* **10:**1093–1095.

DeSesso JM and Jacobson CF (2001) Anatomical and physiological parameters affecting gastrointestinal absorption in humans and rats. *Food Chem Toxicol* **39:**209–28.

Deguchi T, Watanabe N, Kurihara A, Igeta K, Ikenaga H, Fusegawa K, Suzuki N, Murata S, Hirouchi M, Furuta Y (2011) Human pharmacokinetic prediction of UDP-glucuronosyltransferase substrates with an animal scale-up approach. *Drug Metab Dispos* **39:**820–29.

Emi Y, Omura S, Ikushiro S, Iyanagi T (2002) Accelerated degradation of mislocalized UDP–glucuronosyltransferase family 1 (UGT1) proteins in Gunn rat hepatocytes. *Arch Biochem Biophys.*

405:163–9.

Fukuda H, Ohashi R, Ohashi N, Yabuuchi H, Tamai I (2010) Estimation of transporters involved in the hepatobiliary transport of TA-0201CA using sandwich-cultured rat hepatocytes from normal and multidrug resistance-associated protein 2-deficient rats. *Drug Metab Dispos* **38**:1505–13.

Galetin A and Houston JB (2006) Intestinal and hepatic metabolic activity of five cytochrome P450 enzymes: impact on prediction of first-pass metabolism. *J Pharmacol Exp Ther* **318:**1220–9.

Gardiner P, Paine SW. (2011) The impact of hepatic uptake on the pharmacokinetics of organic anions. *Drug Metab Dispos* **39**:1930–8.

Gertz M, Harrison A, Houston JB, and Galetin A (2010) Prediction of human intestinal first-pass metabolism of 25 CYP3A substrates from in vitro clearance and permeability data. *Drug Metab Dispos* **38:**1147–58.

Grime K, Paine SW (2013) Species differences in biliary clearance and possible relevance of hepatic uptake and efflux transporters involvement. *Drug Metab Dispos* **41**:372–8.

Hagenbuch B, Meier PJ (2003) The superfamily of organic anion transporting polypeptides. *Biochim Biophys Acta* **1609**:1–18.

Hisaka A and Sugiyama Y. (1998) Analysis of nonlinear and nonsteady state hepatic extraction with the dispersion model using the finite difference method. *J Pharmacokinet Biopharm* 26: 495–519.

Iwatsubo T, Hirota N, Ooie T, Suzuki H, and Sugiyama Y (1996) Prediction of in vivo drug disposition from in vitro data based on physiological pharmacokinetics. *Biopharm Drug Dispos* **17:**273–310.

Ishizuka H, Konno K, Naganuma H, Sasahara K, Kawahara Y, Niinuma K, Suzuki H, Sugiyama Y (1997) Temocaprilat, a novel angiotensin-converting enzyme inhibitor, is excreted in bile via an ATP-dependent active transporter (cMOAT) that is deficient in Eisai hyperbilirubinemic mutant rats (EHBR). *J Pharmacol Exp Ther* **280**:1304–11.

Jeong EJ, Lin H, and Hu M (2004) Disposition mechanisms of raloxifene in the human intestinal

Caco-2 model. *J Pharmacol Exp Ther* **310:**376–85.

Jeong EJ, Liu Y, Lin H, and Hu M (2005) Species- and disposition model-dependent metabolism of raloxifene in gut and liver: role of UGT1A10. *Drug Metab Dispos* **33:**785–94.

Jia X, Chen J, Lin H, and Hu M (2004) Disposition of flavonoids via enteric recycling: enzyme-transporter coupling affects metabolism of biochanin A and formononetin and excretion of their phase II conjugates. *J Pharmacol Exp Ther* **310:**1103–13.

Kadono K, Akabane T, Tabata K, Gato K, Terashita S, and Teramura T (2010) Quantitative prediction of intestinal metabolism in humans from a simplified intestinal availability model and empirical scaling factor. *Drug Metab Dispos* **38:**1230–7.

Kemp DC, Fan PW, and Stevens JC (2002) Characterization of raloxifene glucuronidation in vitro: contribution of intestinal metabolism to presystemic clearance. *Drug Metab Dispos* **30:**694–700.

Kilford PJ, Stringer R, Sohal B, Houston JB, and Galetin A (2009) Prediction of drug clearance by glucuronidation from in vitro data: use of combined cytochrome P450 and UDP-glucuronosyltransferase cofactors in alamethicin-activated human liver microsomes. *Drug Metab Dispos* **37:**82–9.

Kim MS, Liu DQ, Strauss JR, Capodanno I, Yao Z, Fenyk-Melody JE, Franklin RB, and Vincent SH (2003) Metabolism and disposition of gemfibrozil in Wistar and multidrug resistanceassociated protein 2-deficient TR_ rats. *Xenobiotica* **33:**1027–42.

Köck K, Koenen A, Giese B, Fraunholz M, May K, Siegmund W, Hammer E, Völker U, Jedlitschky G, Kroemer HK, Grube M (2010) Rapid modulation of the organic anion transporting polypeptide 2B1 (OATP2B1, SLCO2B1) function by protein kinase C-mediated internalization. *J Biol Chem* **285**:11336–47.

Kosaka K, Sakai N, Endo Y, Fukuhara Y, Tsuda-Tsukimoto M, Ohtsuka T, Kino I, Tanimoto T, Takeba T, Takahashi M, Kume T (2011) Impact of intestinal glucuronidation on the pharmacokinetics of raloxifene. *Drug Metab Dispos* **39**:1495–502.

Kuroda M, Kobayashi Y, Tanaka Y, Itani T, Mifuji R, Araki J, Kaito M and Adachi Y (2004) Increased hepatic and renal expressions of multidrug resistance-associated protein 3 in Eisai hyperbilirubinuria rats. *J Gastroenterol Hepatol* **19**:146–53.

Lewinsky RH, Smith PA, and Mackenzie PI (2005) Glucuronidation of bioflavonoids by human UGT1A10: structure-function relationships. *Xenobiotica* **35:**117–29.

Li M, Yuan H, Li N, Song G, Zheng Y, Baratta M, Hua F, Thurston A, Wang J, Lai Y (2008) Identification of interspecies difference in efflux transporters of hepatocytes from dog, rat, monkey and human. *Eur J Pharm Sci* **35**:114–26.

Li N, Zhang Y, Hua F, Lai Y (2009) Absolute difference of hepatobiliary transporter multidrug resistance-associated protein (MRP2/Mrp2) in liver tissues and isolated hepatocytes from rat, dog, monkey, and human. *Drug Metab Dispos* **37**:66–73.

Lin JH and Wong BK (2002) Complexities of glucuronidation affecting in vitro in vivo extrapolation. *Curr Drug Metab* **3:**623–46.

Lindstrom TD, Whitaker NG, and Whitaker GW (1984) Disposition and metabolism of a new benzothiophene antiestrogen in rats, dogs and monkeys. *Xenobiotica* **14:**841–47.

Lundquist P, Englund G, Skogastierna C, Lööf J, Johansson J, Hoogstraate J, Afzelius L, Andersson TB (2014a) Functional ATP-binding cassette drug efflux transporters in isolated human and rat hepatocytes significantly affect assessment of drug disposition. *Drug Metab Dispos* **42**:448–58.

Lundquist P, Lööf J, Sohlenius-Sternbeck AK, Floby E, Johansson J, Bylund J, Hoogstraate J, Afzelius L, Andersson TB (2014b) The impact of solute carrier (SLC) drug uptake transporter loss in human and rat cryopreserved hepatocytes on clearance predictions. *Drug Metab Dispos* **42**:469–80.

Luttringer O, Theil FP, Poulin P, Schmitt-Hoffmann AH, Guentert TW, and Lave´ T (2003) Physiologically based pharmacokinetic (PBPK) modeling of disposition of epiroprim in humans. *J Pharm Sci* **92:**1990–2007.

Martignoni M, Groothuis G and de Kanter R (2006) Comparison of mouse and rat cytochrome P450-mediated metabolism in liver and intestine. *Drug Metab Dispos* **34**:1047–54.

Miners JO, Mackenzie PI, and Knights KM (2010) The prediction of drug-glucuronidation parameters in humans: UDP-glucuronosyltransferase enzyme-selective substrate and inhibitor probes for reaction phenotyping and in vitro-in vivo extrapolation of drug clearance and drug-drug interaction potential. *Drug Metab Rev* **42:**196–208.

Mizuma T (2009) Intestinal glucuronidation metabolism may have a greater impact on oral bioavailability than hepatic glucuronidation metabolism in humans: a study with raloxifene, substrate for UGT1A1, 1A8, 1A9, and 1A10. *Int J Pharm* **378:**140–1.

Morikawa A, Goto Y, Suzuki H, Hirohashi T, Sugiyama Y (2000) Biliary excretion of 17beta-estradiol 17beta-D-glucuronide is predominantly mediated by cMOAT/MRP2. *Pharm Res* **17**:546–52.

Mottino AD, Hoffman T, Jennes L, and Vore M (2000) Expression and localization of multidrug resistant protein Mrp2 in rat small intestine. *J Pharmacol Exp Ther* **293:**717–23.

Murata M, Tamai I, Sai Y, Nagata O, Kato H, Sugiyama Y, Tsuji A (1998) Hepatobiliary transport kinetics of HSR-903, a new quinolone antibacterial agent. *Drug Metab Dispos* **26**:1113–9.

Nakagomi-Hagihara R, Nakai D, Kawai K, Yoshigae Y, Tokui T, Abe T, Ikeda T (2006) OATP1B1, OATP1B3, and mrp2 are involved in hepatobiliary transport of olmesartan, a novel angiotensin II blocker. *Drug Metab Dispos* **34**:862–9.

Nakamori F, Naritomi Y, Hosoya K, Moriguchi H, Tetsuka K, Furukawa T, Kadono K, Yamano K, Terashita S, Teramura T (2012) Quantitative prediction of human intestinal glucuronidation effects on intestinal availability of UDP-glucuronosyltransferase substrates using in vitro data. *Drug Metab Dispos* **40**:1771–7.

Nies AT, Schwab M, and Keppler D (2008) Interplay of conjugating enzymes with OATP uptake transporters and ABCC/MRP efflux pumps in the elimination of drugs. *Expert Opin Drug Metab Toxicol* **4:**545–68.

Ninomiya M, Ito K, Horie T. (2005) Functional analysis of dog multidrug resistance-associated protein 2 (Mrp2) in comparison with rat Mrp2. *Drug Metab Dispos* **33**:225–32.

Nishino A, Kato Y, Igarashi T, Sugiyama Y (2000) Both cMOAT/MRP2 and another unknown transporter(s) are responsible for the biliary excretion of glucuronide conjugate of the nonpeptide angiotensin II antagonist, telmisaltan. *Drug Metab Dispos* **28**:1146–8.

Ohno S and Nakajin S (2009) Determination of mRNA expression of human UDPglucuronosyltransferases and application for localization in various human tissues by real-time reverse transcriptase-polymerase chain reaction. *Drug Metab Dispos* **37:**32–40.

Ohtsuki S, Schaefer O, Kawakami H, Inoue T, Liehner S, Saito A, Ishiguro N, Kishimoto W, Ludwig-Schwellinger E, Ebner T, Terasaki T (2012) Simultaneous absolute protein quantification of transporters, cytochromes P450, and UDP-glucuronosyltransferases as a novel approach for the characterization of individual human liver: comparison with mRNA levels and activities. *Drug Metab Dispos* **40**:83–92.

Oleson L and Court MH (2008) Effect of the beta-glucuronidase inhibitor saccharolactone on glucuronidation by human tissue microsomes and recombinant UDP-glucuronosyltransferases. *J Pharm Pharmacol* **60**:1175–82.

Pang KS, Maeng H, and Fan (2009) Interplay of transporters and enzymes in drug and metabolite processing. *Mol Pharm* **6:**1734–55.

Perloff MD, von Moltke LL, and Greenblatt DJ (2004) Ritonavir and dexamethasone induce expression of CYP3A and P-glycoprotein in rats. *Xenobiotica* **34:**133–50.

Powell J, Farasyn T, Köck K, Meng X, Pahwa S, Brouwer KL, Yue W (2014) Novel Mechanism of Impaired Function of Organic Anion-Transporting Polypeptide 1B3 in Human Hepatocytes: Post-Translational Regulation of OATP1B3 by Protein Kinase C Activation. *Drug Metab Dispos* **42**:1964–70.

Reichel C, Gao B, Van Montfoort J, Cattori V, Rahner C, Hagenbuch B, Stieger B, Kamisako T, Meier

PJ (1999) Localization and function of the organic anion-transporting polypeptide Oatp2 in rat liver. *Gastroenterology* **117**:688–95.

Ritter JK (2007) Intestinal UGTs as potential modifiers of pharmacokinetics and biological responses to drugs and xenobiotics. *Expert Opin Drug Metab Toxicol* **3:**93–107.

Rowland A, Gaganis P, Elliot DJ,Mackenzie PI, Knights KM, andMiners JO (2007) Binding of inhibitory fatty acids is responsible for the enhancement of UDP-glucuronosyltransferase 2B7 activity by albumin: implications for in vitro-in vivo extrapolation. *J Pharmacol Exp Ther* **321:**137–47.

Rowland A, Knights KM, Mackenzie PI, and Miners JO (2008) The "albumin effect" and drug glucuronidation: bovine serum albumin and fatty acid-free human serum albumin enhance the glucuronidation of UDP-glucuronosyltransferase (UGT) 1A9 substrates but not UGT1A1 and UGT1A6 activities. *Drug Metab Dispos* **36**:1056–62.

Sakamoto S, Kusuhara H, Horie K, Takahashi K, Baba T, Ishizaki J, Sugiyama Y (2008) Identification of the transporters involved in the hepatobiliary transport and intestinal efflux of methyl 1-(3,4-dimethoxyphenyl)-3-(3-ethylvaleryl)-4-hydroxy-6,7,8-trimethoxy-2-naphthoate (S-8921) glucuronide, a pharmacologically active metabolite of S-8921. *Drug Metab Dispos* **36**:1553–61.

Sathirakul K, Suzuki H, Yasuda K, Hanano M, Tagaya O, Horie T, Sugiyama Y (1993) Kinetic analysis of hepatobiliary transport of organic anions in Eisai hyperbilirubinemic mutant rats. *J Pharmacol Exp Ther* **265**:1301–12.

Shingaki T, Takashima T, Ijuin R, Zhang X, Onoue T, Katayama Y, Okauchi T, Hayashinaka E, Cui Y, Wada Y, Suzuki M, Maeda K, Kusuhara H, Sugiyama Y, Watanabe Y (2013) Evaluation of Oatp and Mrp2 activities in hepatobiliary excretion using newly developed positron emission tomography tracer [11C]dehydropravastatin in rats. *J Pharmacol Exp Ther* **347**:193–202.

Soars MG, Grime K, Sproston JL, Webborn PJ, Riley RJ (2007) Use of hepatocytes to assess the contribution of hepatic uptake to clearance in vivo. *Drug Metab Dispos* **35**:859–65.

Sun H, Zeng YY, and Pang KS (2010) Interplay of phase II enzymes and transporters in futile cycling: influence of multidrug resistance-associated protein 2-mediated excretion of estradiol 17β-D-glucuronide and its 3-sulfate metabolite on net sulfation in perfused TR⁻ and Wistar rat liver preparations. *Drug Metab Dispos* **38:**769–80.

Takekuma Y, Kakiuchi H, Yamazaki K,Miyauchi S, Kikukawa T, Kamo N, Ganapathy V, and Sugawara M (2007) Difference between pharmacokinetics of mycophenolic acid (MPA) in rats and that in humans is caused by different affinities of MRP2 to a glucuronized form. *J Pharm Pharm Sci* **10:**71–85.

von Moltke LL,Greenblatt DJ,Harmatz JS, and Shader RI (1993) Alprazolam metabolism in vitro: studies of human, monkey, mouse, and rat liver microsomes. *Pharmacology* **47:**268–76.

Wang SW, Kulkarni KH, Tang L, Wang JR, Yin T, Daidoji T, Yokota H, and Hu M (2009) Disposition of flavonoids via enteric recycling: UDP-glucuronosyltransferase (UGT) 1As deficiency in Gunn rats is compensated by increases in UGT2Bs activities. *J Pharmacol Exp Ther* **329:**1023–31.

Winiwarter S, Bonham NM, Ax F, Hallberg A, Lennernas H and Karlen A (1998) Correlation of human jejunal permeability (in vivo) of drugs with experimentally and theoretically derived parameters. A multivariate data analysis approach. *J Med Chem* **41:**4939–49.

Wu B, Dong D, Hu M, Zhang S (2013) Quantitative prediction of glucuronidation in humans using the in vitro- in vivo extrapolation approach. *Curr Top Med Chem*. **13**:1343–52.

Xu H, Kulkarni KH, Singh R, Yang Z, Wang SW, Tam VH, and Hu M (2009) Disposition of naringenin via glucuronidation pathway is affected by compensating efflux transporters of hydrophilic glucuronides. *Mol Pharm* **6:**1703–15.

Yamashiro W, Maeda K, Hirouchi M, Adachi Y, Hu Z, Sugiyama Y. (2006) Involvement of transporters in the hepatic uptake and biliary excretion of Valsartan, a selective antagonist of angiotensin II AT1-receptor, in humans. *Drug Metab Dispos* **34**:1247–54.

Yang J, Jamei M, Yeo KR, Tucker GT, and Rostami-Hodjegan A (2007) Prediction of intestinal first-pass drug metabolism. *Curr Drug Metab* **8:**676–684.

Zhang L, Zuo Z, and Lin G (2007) Intestinal and hepatic glucuronidation of flavonoids. *Mol Pharm* **4:**833–845.

Zhou SF, Tingle MD, Kestell P, and Paxton JW (2002) Species differences in the metabolism of the antitumour agent 5,6-dimethylxanthenone-4-acetic acid in vitro: implications for prediction of metabolic interactions in vivo. *Xenobiotica* **32:**87–107.

Papers on publications

I.   Intestinal and hepatic glucuronidation of raloxifene and the other compounds

Kosaka K, Sakai N, Endo Y, Fukuhara Y, Tsuda-Tsukimoto M, Ohtsuka T, Kino I, Tanimoto T, Takeba N, Takahashi M and Kume T (2011) Impact of intestinal glucuronidation on the pharmacokinetics of raloxifene. *Drug Metab Dispos* **39:**1495-1502.

II.   Hepatic uptake and biliary excretion of raloxifene glucuronide and the other compounds

Kosaka K, Watanabe T, Susukida T, Aoki S, Sekine S, Kume T and Ito K (2015) Key determinants of the circulatory exposure for organic anions: the differences in hepatic uptake between multidrug resistance-associated protein 2 (Mrp2) deficient rats and wild-type rats. *Xenobiotica* in press.
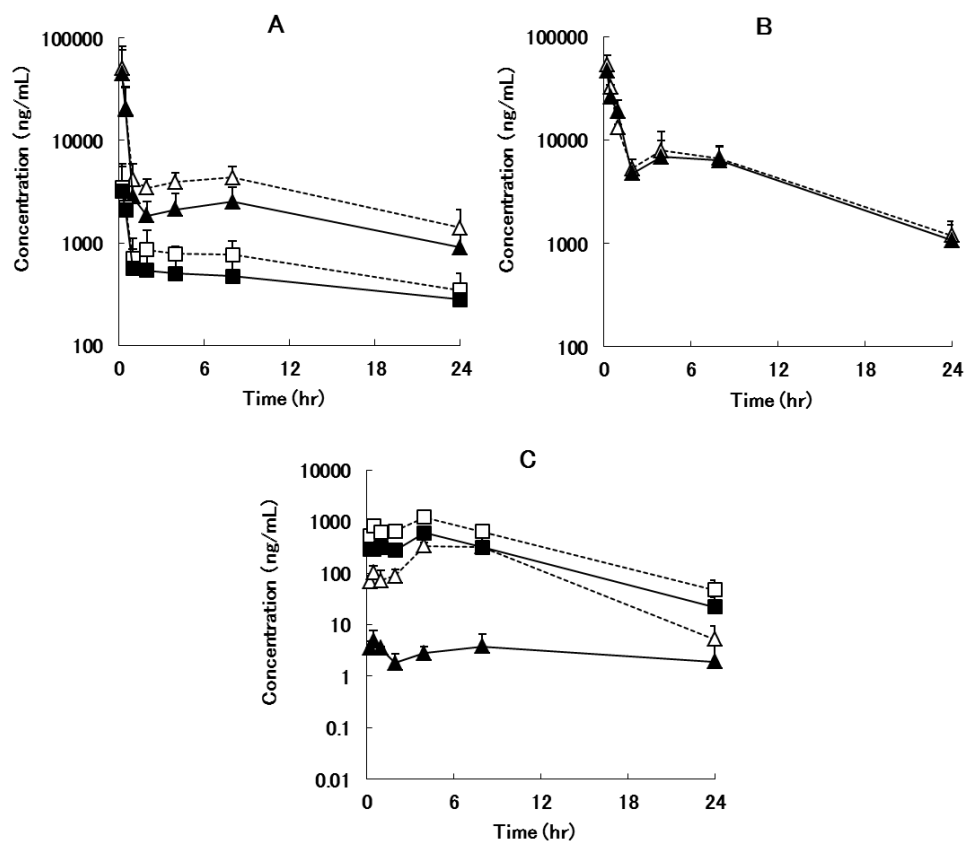
Figure AP-1. Plasma concentration versus time profiles of three compounds after oral administration.

Closed symbols ■, systemic plasma concentrations; open symbols □, portal plasma concentrations.

▲ and △, Parents; ■ and □, their glucuronides.

Gemfibrozil (A), mycophenolic acid (B), and biochanin A (C) were orally administered to SD rats.

Glucuronides of mycophenolic acid were not detectable. Each symbol represents the mean and the

error bars indicate the S.D.
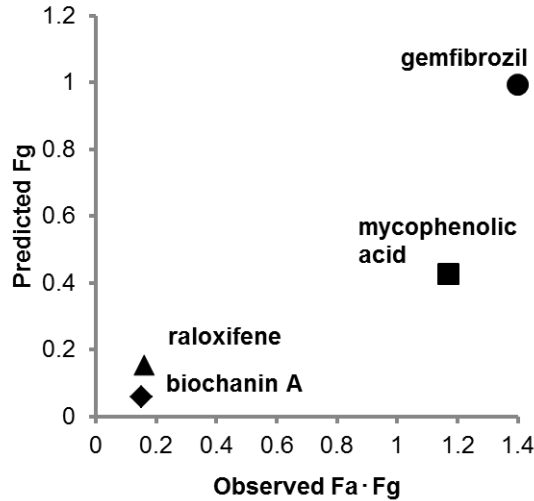
Figure AP-2. Estimation of Fg from in vitro data by Q_{gut} model.

Fg values of four compound were estimated by Q_{gut} model, defined in eqs. A1 and A2 (Yang, 2007):

$$Fg = Q_{gut} / (Q_{gut} + f_{u, g} \cdot CL_{int, u}) \qquad (A1)$$

$$Q_{gut} = Q_{villi} \cdot CL_{perm} / (Q_{villi} + CL_{perm}) \qquad (A2)$$

Q_{gut} means a hybrid parameter consisting of both Q_{villi} (villus blood flow) and cellular permeability (CL_{perm}). CL_{perm} values were calculated from physiochemical properties (Winiwarter, 1998) and the calculated cylindrical surface area of the 60cm segments with radius of 2.2mm, which is enlarged to about 600 times for the feature of microvilli (DeSesso, 2001). Q_{gut} was calculated using CL_{perm} and rat Q_{villi} of 14.4 ml·h^{-1}·kg^{-1} (Davies, 1993). The fraction unbound in the gut ($f_{u, g}$) was assumed to be 1, and intestinal intrinsic clearance ($CL_{int, u}$) obtained by microsomal incubation was scaled up to give $CL_{int, u}$ per gram of tissue by correcting the values of organ weight and the content of microsomal protein (Martignoni, 2006). Predicted Fg values were compared with observed Fa·Fg values.
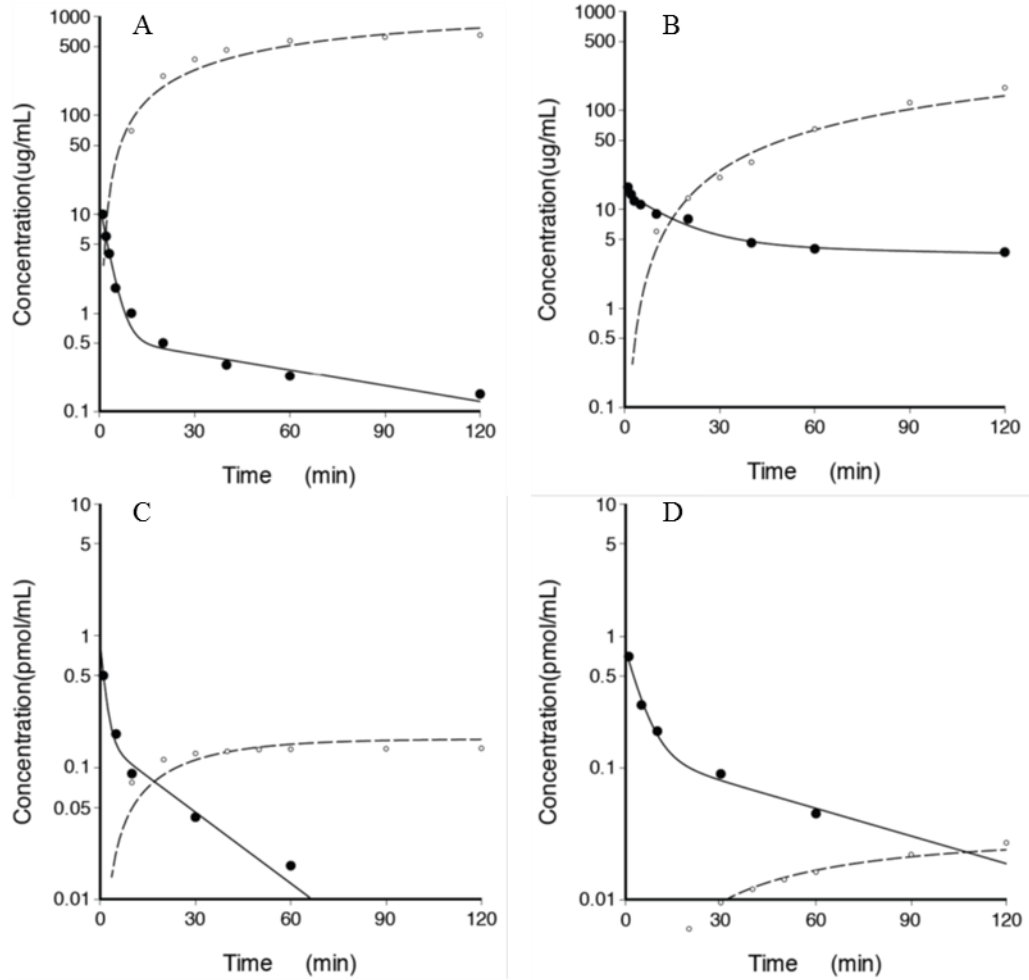
Figure AP-3. Compartmental pharmacokinetic modeling of valsartan and E$_2$17βG in rats.

Compartmental pharmacokinetic modeling of valsartan after the bolus injection was performed in A) SD rats and B) EHBRs using literature data reported by Yamashiro (2006). Similarly, that of E$_2$17βG was performed in C) SD rats and D) EHBRs using literature data reported by Morikawa (2000).

Closed and open symbols represent plasma concentration and cumulative biliary amounts, respectively. Solid and dashed lines represent the simulated curves of plasma concentration and cumulative biliary amounts, respectively.
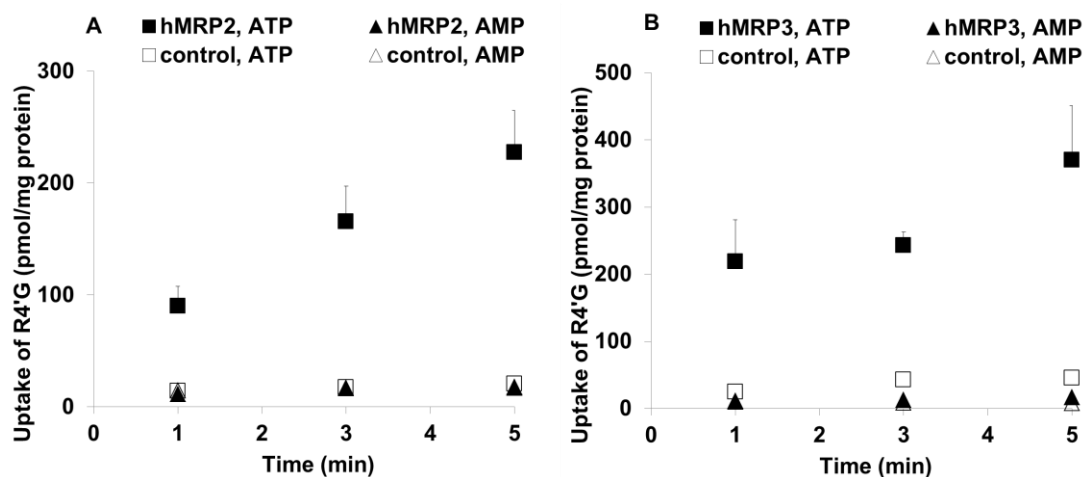
Figure AP-4. Time-dependent transport of [^{14}C] R4'G into human MRP2- and MRP3-expressing membrane vesicles.

Time-dependent uptakes of [^{14}C] R4'G into A) human MRP2- and B) human MRP3-expressing membrane vesicles in the presence of ATP/AMP were presented and compared with those into control membrane vesicles. R4'G is a major metabolite of raloxifene in human. Closed and open symbols represent values of human MRP2/3-expressing membrane vesicles and control membrane vesicles, respectively. Square and triangular symbols represent values of the reactions with ATP and AMP, respectively.
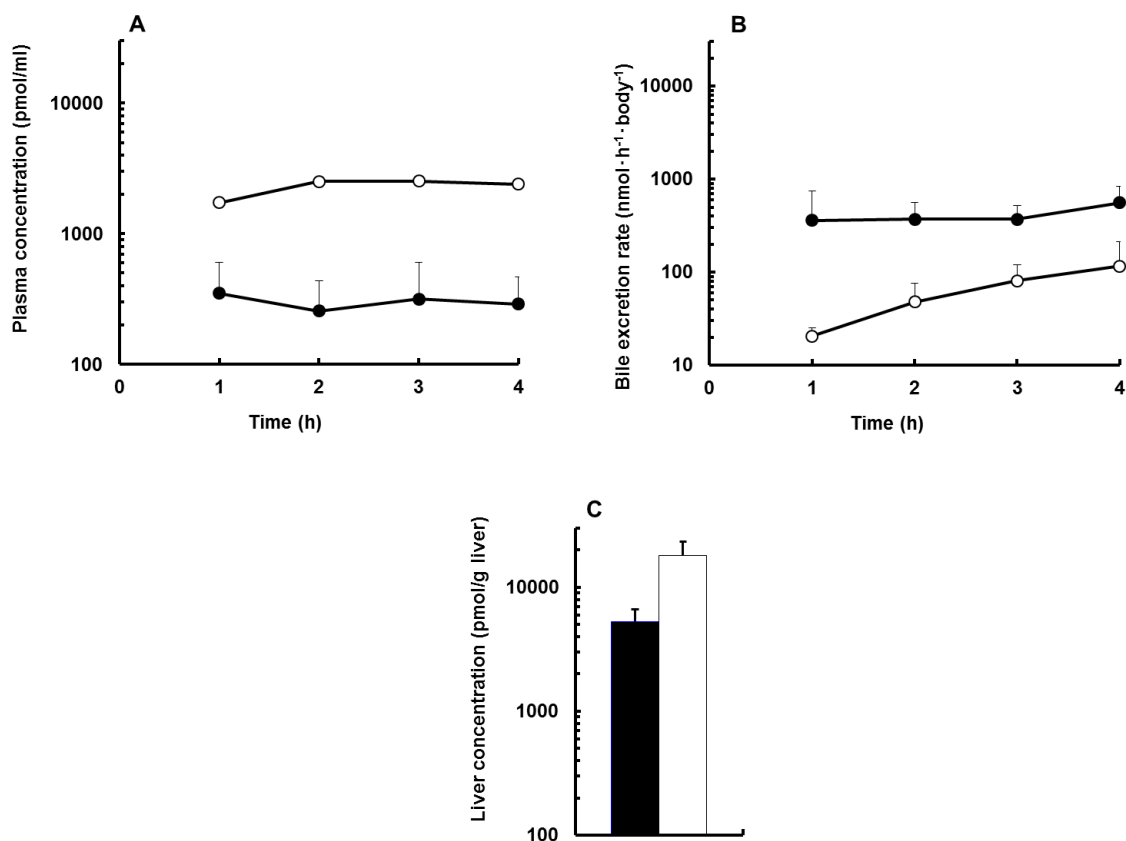
Figure AP-5. Plasma concentration and biliary excretion rate versus time profile and liver concentration of R6G under steady state in rats.

Raloxifene (0.5 μmol$\cdot$h$^{-1}\cdot$body^{-1}) was administered to bile duct-canulated rats (n = 3) by continuous intravenous infusion after bolus injection (0.72 μmol/body). Blood and bile samples were collected at 1, 2, 3, and 4 h after administration, and liver was extracted at the final point. Raloxifene and R6G concentrations in plasma, bile, and liver were measured by LC-MS/MS. A) Closed and open symbols represent plasma concentration of R6G in SD rats and EHBRs, respectively. B) Closed and open symbols represent biliary excretion rate of R6G in SD rats and EHBRs, respectively. C) Closed and open bars represent liver concentration of R6G in SD rats and EHBRs, respectively.
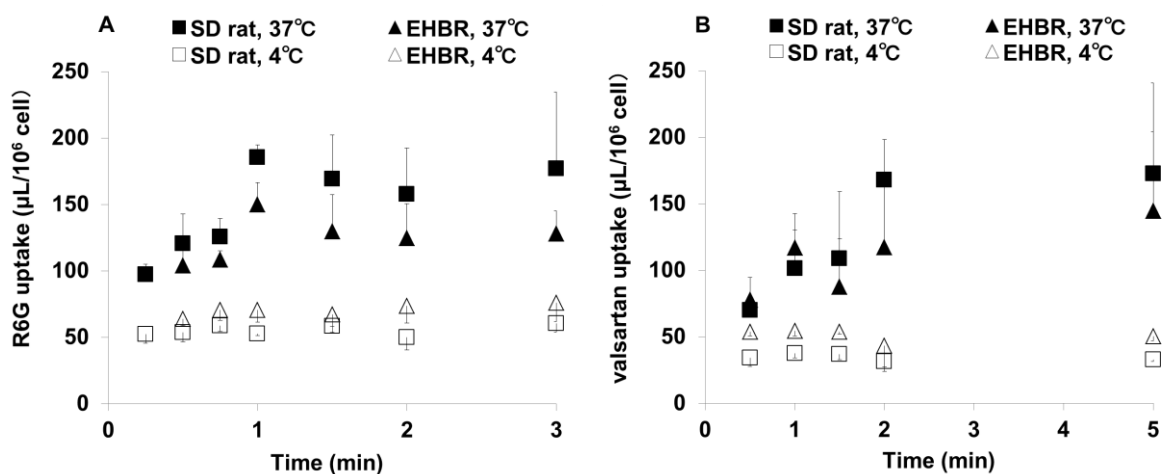
Figure AP-6. Time-dependent uptake of A) R6G and B) valsartan into rat hepatocytes

The hepatocytes isolated from SD rats and EHBRs were suspended (2×10^6 cells/ml) in Krebs-Henseleit (KH) buffer on ice. After pre-incubating the hepatocyte suspension at 37°C for 2 min, the reaction was started by adding the same volume of KH buffer containing A) [^{14}C] R6G (final 0.5 μM) and B) valsartan (final 5 μM). At the designated time, the uptake was terminated by separating the cells from the KH buffer by the centrifugal oil filtration method. As control, the uptake assay was additionally conducted on ice (at 4°C). The concentrations of radioactive and non-labeled compound in cells were measured by a liquid scintillation counter and LC-MS/MS, respectively.
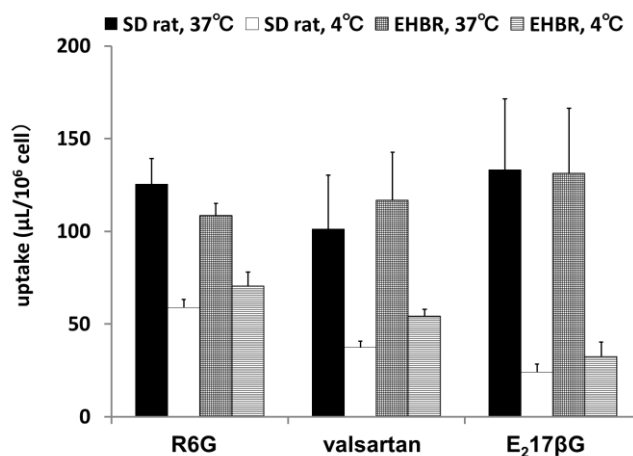
Figure AP-7. Comparison of uptake of three compounds into rat hepatocytes.

The hepatocytes isolated from SD rats and EHBRs were suspended (2×10^6 cells/ml) in KH buffer on ice. After pre-incubating the hepatocyte suspension at 37°C for 2 min, the reaction was started by adding the same volume of KH buffer containing [^{14}C] R6G (final 0.5 μmol/L), valsartan (final 5 μmol/L), and [^{3}H] E$_2$17βG (final 0.1 μmol/L). The uptake was terminated at 0.75, 1, and 2 min, respectively by separating the cells from the KH buffer by the centrifugal oil filtration method. As control, the uptake assay was additionally conducted on ice (at 4°C). The concentrations of radioactive and non-labeled compound in cells were measured by a liquid scintillation counter and LC-MS/MS, respectively.
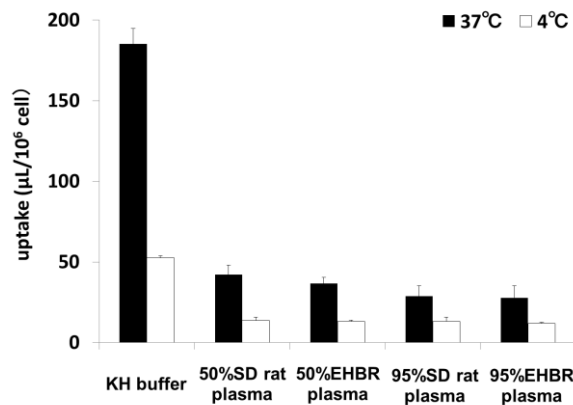
Figure AP-8. Influence of plasma components on the uptake of [14C] R6G uptake into rat hepatocytes.

The hepatocytes isolated from SD rats were suspended (2×10^6 cells/ml) in KH buffer. KH buffer was substituted 50% or 95% by the plasma obtained from SD rats and EHBRs. After pre-incubating these hepatocyte suspensions at 37°C for 2 min, the reaction was started by adding the same volume of KH buffer and the plasma containing [14C] R6G (final 0.5 µmol/L). The uptake was terminated at 1 min by the centrifugal oil filtration method. As control, the uptake assay was additionally conducted on ice (at 4°C). The concentrations of radioactive were measured by a liquid scintillation counter.

Table AP-1. Kinetic parameters of valsartan and $E_2$17βG after bolus injection into SD rats and EHBRs.

Compounds Dose		SD rats	EHBRs	References
[3H]$E_2$17βG	S_1 (*l/kg*)	205 (101)	228 (25)	Morikawa et al.
180 pmol/kg, i.v. bolus	k_e (*1/h*)	0.0152 (0.0188)	0.0608 (0.0074)	(2000)
	k_{12} (*1/h*)	0.557 (0.431)	0.132 (0.022)	
	k_{21} (*1/h*)	0.112 (0.067)	0.0462 (0.008)	
	k_{bile} (*1/h*)	0.0470 (0.0081)	0.00436 (0.00048)	
[3H]valsartan	S_1 (*l/kg*)	80.7 (17.2)	65.9 (6.1)	Yamashiro et al.
1 mg/kg, i.v. bolus	k_e (*1/h*)	0.00001 (−) [1]	0.00001 (−) [1]	(2006)
	k_{12} (*1/h*)	0.380 (0.065)	0.0500 (0.0119)	
	k_{21} (*1/h*)	0.0168 (0.0028)	0.0186 (0.052)	
	k_{bile} (*1/h*)	0.0129 (0.0013)	0.00199 (0.00026)	

1) Fixed parameters

Kinetic parameters of valsartan and $E_2$17βG in SD rats and EHBRs were estimated from the time profiles of concentrations in plasma and bile after intravenous administration as reported by Yamashiro (2006) and Morikawa (2000). Optimized values and fitting standard deviations (in parentheses) are presented.

Table AP-2. Biliary clearance of raloxifene and R6G under steady state in rats.

	SD rats			EHBRs		
Raloxifene						
CL_{tot} (*ml·min^{-1}·kg^{-1}*)	61.5	±	16.6	374	±	64.5
CL_{bile} (*μl·min^{-1}·kg^{-1}*)	1.03	±	0.62	4.20	±	1.04
Kp_{liver}	31.5	±	14.9	101	±	22.2
R6G						
CL_{bile} (*ml·min^{-1}·kg^{-1}*)	4.78	±	1.57	0.283	±	0.271
Kp_{liver}	32.1	±	35.2	7.62	±	2.60

Raloxifene (0.5 μmol·h^{-1}·body^{-1}) was administered to bile duct-canulated rats (n = 3) by continuous intravenous infusion after bolus injection (0.72 μmol/body). Blood and bile samples were collected at 1, 2, 3, and 4 h after administration, and liver was extracted at the final point. Raloxifene and R6G concentrations in plasma, bile, and liver were measured by LC-MS/MS. Biliary clearances of raloxifene and R6G under steady state in rats were estimated based on the concentration in the liver.

Table AP-3. Classified list of Mrp2 substrates: difference in initial distribution between EHBRs and SD rats.

Compounds with initial distribution rate remarkably reduced in EHBRs.
[^{14}C]temocapril (Ishizuka et al., 1997)
[^{3}H]valsartan (Yamashiro et al., 2006)
[^{14}C]S-8921G (Sakamoto et al., 2008)
TA-0201CA (Fukuda et al., 2010)
R6G (this study)
Compounds with initial distribution rate not reduced (or less reduced) in EHBRs.
cefodizime (Sathirakul et al., 1993)
DBSP (Sathirakul et al., 1993)
indocyanine green (Sathirakul et al., 1993)
HSR-903 (Murata et al., 1998)
[^{14}C]telmisartan (Nishino et al., 2000)
[^{3}H]E$_2$17βG (Morikawa et al., 2000)
[^{14}C]olmesartan (Nakagomi-Hagihara et al., 2006)
[^{11}C]dehydropravastatin (Shingaki et al., 2014)

Pharmacokinetic data of organic anions including plasma and bile concentration in SD rats and EHBRs were collected and classified based on the difference in initial distribution between these rats. All compounds collected show reduced bile excretion rates in EHBRs compared to those in SD rats due to hereditary deficiency of Mrp2, whereas they have different profiles in alteration of initial distribution between these rats. A decrease in initial distribution rate in EHBRs is presumably caused by reduction of hepatic uptake clearance. They are classified to two types: compounds with initial distribution rate remarkably reduced or not (less reduced) in EHBRs.

List of Tables

List of Appendix Figures and Tables

74

List of Abbreviations

AUC: area under the curve

BSA: bovine serum albumin

C: Concentration

CL_b: hepatic blood clearance

CL_{int}: intrinsic clearance

$CL_{int, h}$: whole-body clearance estimated from the data using liver microsomes

$CL_{int, iv}$: hepatic clearance values after intravenous administration

$CL_{int, po}$: hepatic clearance values after oral administration

CL_{tot}: total clearance

$CL_{int, u}$: intrinsic clearance corrected by unbound fraction

$f_{u, mic}$: unbound fraction in microsomal incubation

$f_{u, p}$: unbound fraction in plasma

P450: cytochrome P450

$E_2 17\beta G$: estradiol-17β-glucuronide

EHBR: Eisai hyperbilirubinemic rat

Fa: absorbed fraction

Fg: intestinal availability

Fh: hepatic availability

k_{12}: hepatic uptake rate constant

k_{21}: sinusoidal efflux rate constant

k_{bile}: biliary excretion rate constant

k_e: elimination rate constant

IS: internal standard

IVIVC: in vivo-in vitro correlation

LC-MS/MS: liquid chromatography/tandem mass spectrometry

MRP/Mrp: multidrug resistance-associated protein

NADPH: nicotinamide adenine dinucleotide phosphate

NCE: new chemical entity

P-gp: P-glycoprotein

PBS: phosphate buffer solution

Q_h: hepatic blood flow

Q_{pv}: portal vein blood flow

Q_{villi}: villus blood flow

R4'G: Raloxifene-4'-glucuronide (major metabolite of raloxifene in humans)

R6G: Raloxifene-6-glucuronide (major metabolite of raloxifene in rats)

R_b: blood/plasma concentration ratio

SD: Sprague-Dawley

S_1: systemic volume of distribution

UDPGA: UDP-glucuronic acid

UGT/Ugt: UDP-glucuronosyltransferase

UPLC: ultra-performance liquid chromatography

Vd_{ss}: steady state volume of distribution

Acknowledgements

Reviewers

This work, for the Degree of Doctor of Pharmacy, was examined by following reviewers authorized by Graduate School of Pharmaceutical Sciences, Chiba University.

Dr. Kan Chiba, Professor of Chiba University

(Faculty of Pharma Pharmaceutical Sciences), Chief Reviewer.

Dr. Yasushi Arano, Professor of Chiba University

(Faculty of Pharma Pharmaceutical Sciences), Reviewer.

Dr. Akihiro Hisaka, Professor of Chiba University

(Faculty of Pharma Pharmaceutical Sciences), Reviewer.